UNIVERSIDADE ESTADUAL PAULISTA “JÚLIO DE MESQUITA FILHO”
FACULDADE DE ENGENHARIA – CÂMPUS DE ILHA SOLTEIRA
PROGRAMA DE PÓS-GRADUAÇÃO EM ENGENHARIA ELÉTRICA

PABLO MAURICIO PORTILLA HERNÁNDEZ

Multichannel functional electrical stimulation-assisted cycling (FES-Cycling) triggered by crank angular ranges and personalisation using artificial intelligence

Ilha Solteira
2026

PABLO MAURICIO PORTILLA HERNÁNDEZ

Multichannel functional electrical stimulation-assisted cycling (FES-Cycling) triggered by crank angular ranges and personalisation using artificial intelligence

Thesis submitted to the Faculty of Engineering, Ilha Solteira Campus – UNESP, in partial fulfilment of the requirements for the degree of Doctor of Philosophy in Electrical Engineering.

Area of concentration: Automation.

Prof. Dr Marcelo Augusto Assunção Sanches
Supervisor

Ilha Solteira

2026

FICHA CATALOGRÁFICA
Desenvolvido pelo Serviço Técnico de Biblioteca e Documentação

H532m

Hernández, Pablo Mauricio Portilla.
Multichannel functional electrical stimulation-assisted cycling (fes-cycling) triggered by crank angular ranges and personalisation using artificial intelligence / Pablo Mauricio Portilla Herández. -- Ilha Solteira: [s.n.], 2026
98 f. : il.

Tese (Doutorado em Engenharia Elétrica) - Universidade Estadual Paulista (UNESP), Faculdade de Engenharia, Ilha Solteira. Área de conhecimento: Automação, 2026

Orientador: Marcelo Augusto Assunção Sanches

Inclui bibliografia

1. Fes-cycling. 2. Multichannel functional electrical stimulation. 3. Inertial sensor. 4. Angular stimulation ranges. 5. Stimulation personalisation. 6. Artificial intelligence.

Sandra Montibeller - CRB-8/060/2025

IMPACTO POTENCIAL DESTA PESQUISA

Esta pesquisa desenvolve uma plataforma de ciclismo assistido por eletroestimulação funcional, integrando sensoriamento inercial, acionamento por faixas angulares e inteligência artificial. A proposta contribui para tecnologias assistivas de reabilitação, saúde e bem-estar (ODS 3) e inovação tecnológica (ODS 9).

POTENTIAL IMPACT OF THIS RESEARCH

This research develops a functional electrical stimulation-assisted cycling platform integrating inertial sensing, angular-range triggering and artificial intelligence. The proposed approach contributes to assistive rehabilitation technologies, health and well-being (SDG 3) and technological innovation (SDG 9).

UNIVERSIDADE ESTADUAL PAULISTA

Câmpus de Ilha Solteira

CERTIFICADO DE APROVAÇÃO

TÍTULO DA TESE: CICLISMO ASSISTIDO POR ELETROESTIMULAÇÃO FUNCIONAL MULTICANAL (FES-CYCLING) GATILHADA POR FAIXAS ANGULARES DA PEDIVELA E PERSONALIZAÇÃO POR INTELIGÊNCIA ARTIFICIAL

AUTOR: PABLO MAURICIO PORTILLA HERNANDEZ
ORIENTADOR: MARCELO AUGUSTO ASSUNÇÃO SANCHES

Aprovado como parte das exigências para obtenção do Título de Doutor em Engenharia Elétrica, área: Automação pela Comissão Examinadora:

gov.br
Documento assinado digitalmente
MARCELO AUGUSTO ASSUNCAO SANCHES
Data: 01/07/2026 19:18:55-0300
Verifique em https://validar.iti.gov.br

Prof. Dr. MARCELO AUGUSTO ASSUNÇÃO SANCHES (Participaçao Presencial)
Departamento de Engenharia Elétrica / Faculdade de Engenharia de Ilha Solteira - UNESP/FEIS

gov.br
Documento assinado digitalmente
APARECIDO AUGUSTO DE CARVALHO
Data: 30/07/2026 18:27:34-0300
Verifique em https://validar.iti.gov.br

Prof. Dr. APARECIDO AUGUSTO DE CARVALHO (Participaçao Presencial)
Departamento de Engenharia Eletrica / Faculdade de Engenharia de Ilha Solteira - UNESP/FEIS (Aposentado)

gov.br
Documento assinado digitalmente
JOAQUIM MIGUEL MAIA
Data: 03/07/2026 14:46:08-0300
Verifique em https://validar.iti.gov.br

Prof. Dr. JOAQUIM MIGUEL MAIA (Participaçao Presencial)
Departamento Acadêmico de Eletronica - DAELN / Universidade Tecnológica Federal do Paraná - UTFPR

gov.br
Documento assinado digitalmente
PERCY NOHAMA
Data: 03/07/2026 17:57:45-0300
Verifique em https://validar.iti.gov.br

Prof. Dr. PERCY NOHAMA (Participaçao Virtual)
Programa de Pós-graduação em Tecnologia em Saúde / Pontífica Universidade Católica do Paraná - PUCPR

gov.br
Documento assinado digitalmente
JOSIVALDO GODOY DA SILVA
Data: 03/07/2026 09:59:13-0300
Verifique em https://validar.iti.gov.br

Prof. Dr. JOSIVALDO GODOY DA SILVA (Participaçao Virtual)
Centro de Ciências Exatas e Tecnologia / Universidade Federal de Mato Grosso do Sul - UFMS

Ilha Solteira, 25 de junho de 2026.

To my parents, Jaime Portilla and Alicia Hernández (in memoriam), my godmother Laura Montesdeoca (in memoriam), and my teacher Diana Cifuentes. I dedicate this thesis.

ACKNOWLEDGEMENTS

The completion of this PhD marks the culmination of a long and challenging path, built over years of continuous learning. I recognise that the most difficult moments of this journey were eased by the presence, support and affection of many people. Although this thesis bears my name on its cover, its existence is the result of a truly shared endeavour. Not a single line of this work was written in isolation; every step, every challenge overcome and every discovery carries the contribution and generosity of those who extended a helping hand, shared my anxieties and believed in me along the way. To all those who transformed this journey into a collective experience, I express my deepest gratitude.

To my father, Jaime, I express my deepest gratitude for everything you have done for me and for my education. Your example, your efforts and your unwavering faith in the transformative power of education were fundamental in enabling me to reach this point. You always encouraged me to do my best and motivated me in the face of every academic challenge. Much of the strength I found to follow this path—as well as many of the values that shaped the person and professional I have become—was born from the lessons and example I received from you.

To my mother, Alicia, whose memory I carry always in my heart, I wish to express my deepest gratitude. From my earliest years, you nurtured my curiosity, encouraged me to study and taught me always to give the very best of myself. You believed with all your heart in the transformative power of education and encouraged us to overcome our limitations. You dreamed that your children would become engineers; now, I feel that I have carried that dream further than either of us could ever have imagined—a dream that you planted in me. I hope I have honoured your efforts and made you proud, wherever you may be. All the determination that sustained me throughout this journey grew out of your teachings, the demanding yet deeply loving way in which you guided us, and the unwavering faith you always had in me.

To my godmother, Laura, whose memory I carry always in my heart, I wish to express my deepest gratitude for opening the doors of your home and your heart to us during a decisive stage of our lives. Your support was far more than an expression of affection; it was a generous and selfless commitment to our future. With time, I came to understand that behind every firm word and every demand lay immense love and the sincere wish for my brother and me to move forward in life. You taught us to value education, to work hard and never to settle for less than we were capable of achieving. As I bring this chapter to a close, I recognise that this achievement also bears the mark of your care, your sacrifices and the trust you always placed in us. I hope I have honoured you and that, wherever you may be, you can feel proud of the path I have taken.

To my dear teacher, Diana, I wish to express my deepest and most sincere thanks. With you, I learnt to look beyond my own limitations and to dream without fear. You taught me that great goals only have true value when they are pursued with integrity, respect and the humility to extend a hand to others. On the most difficult days of this PhD, when tiredness and doubt weighed heavily, I returned more than once to the memory of your classroom and to the words with which you encouraged me to believe in myself. Your influence was one of the first seeds from which this journey grew. Thank you for teaching the child I was that no dream, however distant it may seem, is beyond our reach.

To my brother and friend, Eduardo, thank you for showing me that no physical distance has ever managed to separate us. With you, I took my first steps into the world of curiosity. When we were children, we would take apart remote-controlled toys to discover what was inside. Sometimes we managed to understand how their circuits worked; at other times, we ended up with a few pieces left over. Nevertheless, it was through those little adventures that my fascination with electronics and with discovering how things work was born. You were also by my side whenever I needed the courage to push beyond my own limits. Thank you for being my point of reference, for recognising my potential even when the world seemed to doubt me, and for teaching me to look at life with simplicity—that unique way you have of finding solutions, even when everyone else is still trying to work out what the problem was. This achievement is as much yours as it is mine, because your unconditional support continues to give me the strength and confidence to go ever further.

To Martine, my deepest gratitude for having been a beacon of kindness and a safe harbour throughout this journey. Your integrity, generosity and academic brilliance have always been, for me, an inspiring example and a constant invitation to grow. I am profoundly grateful for the warmth with which you welcomed me, for the bond of affection and trust we have built, and for the way you made me feel truly at home. In you, I found not only inspiration and guidance, but also the warmth of family and the companionship of a dear friend. Your generous advice and unwavering faith in my potential have helped me look towards the future with greater courage and wisdom.

To Sheila, my partner, I offer my warmest thanks for walking alongside me throughout this journey. Thank you for sharing everyday life with me, with its small victories and most difficult moments—those things that never appear in a thesis, but quietly sustain everything. Your care, words of encouragement and understanding in the face of my absences gave me the strength to continue. I am grateful for all you have taught me along the way, for helping me grow as a person and for the generosity that, in so many ways, has also become part of this work. For everything we have experienced and built together during this chapter, I offer you my deepest gratitude. This achievement is, in so many ways, yours too.

To my nieces, Alicia, Alejandra, Ruth and Celeste, I would also like to make room for you in these pages, with all my affection. As I reach the end of this PhD, I find myself reflecting on how the desire to learn and discover often begins with a simple, open outlook, filled with wonder at the world. In the curiosity, spontaneity and joy with which children approach the unknown, I find a beautiful reminder that we should never lose the ability to marvel at new things, to ask questions and to keep seeking answers. This attitude, so natural in childhood and something we sometimes leave behind as we grow older, lies at the heart of all research. I hope that each of you will always preserve that light, follow your own path with courage and find reasons in life to keep learning, dreaming and discovering. Although time and circumstances may change, you will always hold a special place in my heart.

To my supervisor and friend, Prof. Dr Marcelo Augusto Assunção Sanches, I wish to express my deepest and most sincere gratitude. From the moment you opened the doors of UNESP to me, your presence was decisive in allowing me to start again and rebuild my path. Your dedication was never limited to the technical aspects of research; your guidance was always accompanied by genuine human support, especially during the moments of greatest vulnerability. I thank you for the patience and generosity with which you shared your knowledge, for your friendship and for the good humour that made the challenges of this journey lighter. Through complex projects, difficulties overcome and shared learning, we built a partnership grounded in trust, respect and constant encouragement. More than guiding the development of a researcher, you contributed profoundly to my development as a professional and as a person. Your leadership, friendship and confidence in me will remain fundamental references throughout my career.

To Prof. Dr Aparecido Augusto de Carvalho, I express my sincere gratitude for the welcome and opportunity you offered me when I began my journey at UNESP and at the Laboratory of Instrumentation and Biomedical Engineering (LIEB). At that time, when everything was still new to me, your receptiveness and trust were essential in enabling me to take my first steps in postgraduate studies with greater confidence. By opening the doors of the laboratory to me, you made possible the beginning of a journey marked by extensive learning and achievements built over the following years. I deeply appreciate the generosity with which you welcomed me and the trust you placed in me.

To Prof. Dr Adalberto Vieira Corazza, I express my sincere gratitude for the partnership built through different projects and for bringing together the knowledge of engineering and medicine in our work. I thank you for sharing your experience in the field of health and for carefully and patiently guiding the experimental stages. Your willingness to listen to new ideas, your enthusiasm and your good humour made the challenges lighter and turned each experience into an opportunity for learning. I am deeply grateful for the time, dedication and knowledge you shared so generously, all of which contributed

significantly to this research.

To the LIEB family, I offer my eternal affection for transforming a workplace into a true home of companionship and learning. Thank you for your daily companionship, your patience in sharing knowledge and the helping hand you always extended on difficult days. The friendship and unity we cultivated around the laboratory benches and through our experiments made the research journey much lighter, more enriching and more humane.

To the professors of the Department of Electrical Engineering, the staff of FEIS/UNESP and the Postgraduate Programme in Electrical Engineering, I express my gratitude for your institutional support, your daily commitment and for sustaining the conditions in which excellent science and human development can flourish.

To the members of the examining committee, I express my respectful gratitude. I thank you for the time devoted to the rigorous reading of this work and for your valuable contributions. Your reflections and attentive review were essential in refining and consolidating this thesis.

Finally, I hold on to the certainty that this achievement belongs not only to me. It also belongs to all those who walked alongside me, believed in me, extended a helping hand during difficult moments and shared every stage of this journey with me. I carry with me not only the knowledge I have acquired, but also the affection, examples and lessons of everyone who was part of this path. To each and every one of you, from the bottom of my heart, my most sincere thanks.

This study was carried out with the support of the Brazilian Coordination for the Improvement of Higher Education Personnel (CAPES), Finance Code 001.

"If I have seen further, it is by standing
on the shoulders of giants."
Isaac Newton

"Life is like riding a bicycle; to maintain
one's balance, one must keep moving."
Albert Einstein

RESUMO

Esta tese apresenta o desenvolvimento e a avaliação experimental de um sistema de FES-Cycling com estimulação elétrica funcional multicanal baseada na posição angular da pedivela. A proposta concentra-se na sincronização entre a posição angular da pedivela e o acionamento dos canais de estimulação, com o objetivo de tornar a aplicação da FES mais rastreável, configurável e adequada ao ciclo de pedalada. A plataforma foi implementada em uma bicicleta reclinada de três rodas, integrando sensor inercial na pedivela, unidade central de controle, interface manual de ajuste da intensidade, parada de emergência, módulos FES multicanais e sistema de registro dos dados experimentais. A metodologia experimental foi estruturada para registrar a posição angular da pedivela, as faixas angulares de estimulação e os parâmetros associados aos ensaios. Os dados foram organizados em arquivos experimentais e processados para extração de métricas cinemáticas, incluindo número de ciclos completos, cadência, periodicidade angular e escore global de desempenho. Essas métricas foram utilizadas para comparar diferentes configurações de estimulação e apoiar a personalização das faixas angulares de estimulação. Como etapa complementar, foi aplicada uma rede neural do tipo Perceptron Multicamadas (MLP), em modo offline, para estimar novas configurações a partir dos descritores cinemáticos extraídos dos ensaios. A rede neural não atua como controlador autônomo em tempo real, mas como ferramenta de apoio à seleção de faixas angulares de estimulação candidatas. Entre os testes iniciais, a melhor configuração apresentou 9 ciclos completos, cadência média de 13,4 rpm e escore cinemático de 0,8407. Após a aplicação das configurações sugeridas pela rede neural, foram obtidos 11 ciclos completos, com cadências de 15,2 e 15,8 rpm e escores cinemáticos de 0,9515 e 0,9892, respectivamente. Em relação ao melhor teste inicial, a cadência média aumentou aproximadamente 18%. Como a amplitude máxima de estimulação foi mantida em 34 mA, os resultados indicam que as alterações nas faixas angulares de estimulação estiveram associadas à melhora do desempenho cinemático da pedalada nas condições experimentais avaliadas. Os resultados demonstram que a plataforma desenvolvida permite sincronizar a estimulação FES com a posição angular da pedivela, registrar os ensaios de forma rastreável e comparar diferentes configurações com base em indicadores quantitativos. A contribuição principal da tese está na integração entre sensoriamento inercial, acionamento angular da FES, aquisição estruturada de dados e suporte computacional à personalização das faixas angulares de estimulação, oferecendo uma infraestrutura experimental de menor complexidade instrumental para estudos de FES-Cycling orientados por dados, sem depender de medição direta de torque ou de modelagem biomecânica completa.

Palavras-chave: FES-Cycling; estimulação elétrica funcional multicanal; sensor inercial; faixas angulares de estimulação; personalização da estimulação; inteligência artificial.

ABSTRACT

This thesis presents the development and experimental evaluation of an FES-Cycling system with multichannel functional electrical stimulation based on the angular position of the crank. The proposed approach focuses on synchronising the crank angular position with the activation of the stimulation channels, with the aim of making the application of FES more traceable, configurable and better aligned with the pedalling cycle. The platform was implemented on a three-wheeled recumbent bicycle and integrates an inertial sensor mounted on the crank, a central control unit, a manual interface for stimulation-current-amplitude adjustment, an emergency stop, multichannel FES modules and an experimental data-logging system. The experimental methodology was structured to record the crank angular position, the stimulation angular ranges and the parameters associated with each trial. The data were organised into experimental files and processed to extract kinematic metrics, including the number of complete cycles, cadence, angular periodicity and a kinematic score. These metrics were used to compare different stimulation configurations and to support the personalisation of the stimulation angular ranges. As a complementary step, a multilayer perceptron (MLP) neural network was applied offline to estimate new configurations from the kinematic descriptors extracted from the trials. The neural network does not operate as an autonomous real-time controller, but rather as a tool supporting the selection of candidate stimulation angular ranges. Among the initial trials, the best configuration achieved 9 complete cycles, a mean cadence of 13.4 rpm and a kinematic score of 0.8407. After applying the configurations suggested by the neural network, 11 complete cycles were achieved, with cadences of 15.2 and 15.8 rpm and kinematic scores of 0.9515 and 0.9892, respectively. Compared with the best initial trial, the mean cadence increased by approximately 18%. As the maximum stimulation amplitude was maintained at 34 mA during these trials, the results indicate that changes in the stimulation angular ranges were associated with improved kinematic performance under the experimental conditions evaluated. The results show that the developed platform can synchronise FES with the angular position of the crank, record trials in a traceable manner and compare different stimulation configurations using quantitative indicators. The main contribution of this thesis lies in the integration of inertial sensing, angular FES activation, structured data acquisition and computational support for the personalisation of stimulation angular ranges, providing experimental infrastructure with lower instrumentation complexity for data-driven FES-Cycling studies without relying on direct torque measurement or complete biomechanical modelling.

Keywords: FES-Cycling; multichannel functional electrical stimulation; inertial sensor; stimulation angular ranges; stimulation personalisation; artificial intelligence.

LIST OF FIGURES

LIST OF TABLES

LIST OF ABBREVIATIONS AND ACRONYMS

BNO055	BNO055 inertial measurement unit
CAAE	Brazilian ethics-review protocol identifier
CNS	Central nervous system
DAC	Digital-to-analogue converter
DC–DC	Direct-current-to-direct-current converter
EMG	Electromyography
ESP32	ESP32 microcontroller
FES	Functional electrical stimulation
FES-Cycling	Functional electrical stimulation-assisted cycling
IMU	Inertial measurement unit
SCI	Spinal cord injury
MLP	Multilayer Perceptron
MMG	Mechanomyography
OIDA	Optimal Interval Detection Algorithm
PI	Proportional–integral
PID	Proportional–integral–derivative
RL	Reinforcement learning
SDG	Sustainable Development Goals

LIST OF SYMBOLS

θ	Crank angular position, in degrees or radians as appropriate
$\theta(t)$	Instantaneous crank angular position at time t
$\Delta\theta$	Approximate angular displacement associated with the electromechanical delay
$\theta_{i,m}$	Initial angle of the stimulation range for muscle group m
$\theta_{f,m}$	Final angle of the stimulation range for muscle group m
$\boldsymbol{\theta}_{m,i}$	Vector containing the initial and final limits of the angular range for muscle m in trial i
F_m	Stimulation angular range associated with muscle group m
$u_m(\theta)$	Channel activation logic function associated with muscle group m
$S_1(t)$	Logic signal associated with the positive phase of the H-bridge
$S_2(t)$	Logic signal associated with the negative phase of the H-bridge
S_3	Control signal associated with the current-amplitude reference
$I_i(t)$	Stimulation current applied to channel i
$I_m(t)$	Stimulation current applied to the channel associated with muscle group m
$I_{\mathrm{ref},i}$	Reference current of channel i
$I_{\mathrm{ref},m}(t)$	Reference current of the channel associated with muscle group m
$f_i(\cdot)$	Calibration function relating the command to the current delivered by the output stage
$\tau_{\mathrm{net}}(\theta)$	Net torque as a function of angular position
$\tau_{\mathrm{active}}(\theta)$	Torque measured during an active stimulated cycle
$\tau_{\mathrm{passive}}(\theta)$	Torque measured during a passive unstimulated cycle
t	Time
Δt	Electromechanical delay between the electrical pulse and the muscular response

T_{trial}	Total trial duration, in seconds
t_{initial}	Initial trial time
t_{final}	Final trial time
N	Total number of samples or trials, as appropriate
n	Number of samples considered in the statistical calculation
N_{cycles}	Number of complete pedalling cycles
$\omega(t)$	Instantaneous crank angular velocity
$C(t)$	Instantaneous cadence
C_k	Instantaneous cadence at sample k
$\overline{C}$	Mean cadence
C_{rpm}	Mean cadence estimated from the cycle count, in revolutions per minute
$\overline{C}_{\text{inst}}$	Mean instantaneous cadence
σ_C	Cadence standard deviation
CV_C	Cadence coefficient of variation, in per cent
P_θ	Angular periodicity metric between successive cycles
E_α	Kinematic indicator associated with variation in angular acceleration
R_{dz}	Proportion of time spent in the low-velocity zone
S_θ	Overall angular performance index
R_ω	Crank angular-velocity regularity indicator
$\mathcal{D}$	Supervised dataset used for modelling
$\mathbf{x}_i$	Model input vector for trial i
$\mathbf{y}_i$	Desired model output vector for trial i
$\hat{\mathbf{y}}_i$	Model-estimated output vector for trial i
$\hat{\mathbf{y}}_{\text{new}}$	Estimated output vector for a new experimental input
$\mathbf{x}_{\text{new}}$	Input vector for a new experimental condition
$f_{\mathbf{W}}(\cdot)$	Regression function represented by the neural network with parameters $\mathbf{W}$

$\mathbf{W}$	Set of model weights
$\mathbf{W}^{\star}$	Set of weights obtained after training
$\mathcal{L}(\mathbf{W})$	Loss function used in supervised training
d_y	Dimension of the model output vector
$\mathbf{h}_{1,i}$	Activation vector of the first hidden layer
$\mathbf{h}_{2,i}$	Activation vector of the second hidden layer
ϕ_1, ϕ_2	Activation functions of the hidden layers
$\mathbf{W}_1$, $\mathbf{W}_2$, $\mathbf{W}_3$	Weight matrices of the neural-network layers
$\mathbf{b}_1$, $\mathbf{b}_2$, $\mathbf{b}_3$	Bias vectors of the neural-network layers
p_Q, p_G, p_H	Relative activation percentages of the quadriceps, gluteal and hamstring muscle groups
w_{rpm}	Weight associated with cadence in the angular score
w_{stab}	Weight associated with cadence stability in the angular score
w_{per}	Weight associated with angular periodicity in the angular score
w_{α}	Weight associated with angular-acceleration variation in the angular score
w_{dz}	Weight associated with time spent in the low-velocity zone in the angular score
$\widetilde{C}_{\mathrm{rpm}}$	Normalised cadence
$\widetilde{\sigma}_C$	Normalised cadence deviation
$\widetilde{P}_{\theta}$	Normalised angular periodicity
$\widetilde{E}_{\alpha}$	Normalised energy associated with angular acceleration
$\widetilde{R}_{\mathrm{dz}}$	Normalised proportion of time spent in the low-velocity zone
Q	Quadriceps
G	Gluteal muscles
H	Hamstrings
RQ	Right quadriceps

RG	Right gluteal muscles
RH	Right hamstrings
LQ	Left quadriceps
LG	Left gluteal muscles
LH	Left hamstrings
Hz	hertz, unit of frequency
mA	milliampere, unit of electric current
μs	microsecond, unit of time
rpm	revolutions per minute

CONTENTS

1 INTRODUCTION

1.1 BACKGROUND

Spinal cord injury is among the neurological conditions that most severely affect an individual's functional capacity and may result in partial or complete loss of voluntary movement below the level of the injury. In addition to motor limitations, reduced mobility favours the development of musculoskeletal, cardiovascular and metabolic changes, including muscle atrophy, loss of bone mass, reduced cardiorespiratory fitness and impaired quality of life.

In this context, various therapeutic strategies have been investigated to minimise the effects of physical inactivity and preserve remaining neuromuscular function. Functional electrical stimulation (FES) is among these strategies. It consists of the controlled delivery of electrical pulses to excitable tissues to induce coordinated muscle contractions. In neuromotor rehabilitation, FES enables the artificial activation of muscle groups in the presence of reduced or absent voluntary motor control and is used in activities such as assisted gait, hand grasping, standing and therapeutic cycling (Peckham and Knutson, 2005; Lynch and Popovic, 2008).

In the context of spinal cord injury, neuromuscular electrical stimulation has been investigated as a means of assisting locomotion and gait training in individuals with motor impairment. Previous studies examined neuromuscular electrical stimulation systems for individuals with paraplegia or tetraplegia resulting from spinal cord injury (Junior, 1992; Klein, 2001). Subsequent studies evaluated gait training with neuromuscular electrical stimulation in paraplegic patients and analysed electromyographic activity during the process (Cacho, 2004). Urodynamic responses have also been investigated in patients undergoing electrical stimulation for motor rehabilitation after high-level spinal cord trauma (Pedro *et al.*, 2005; D'Ancona *et al.*, 2010).

One of the most established applications of this technology is FES-Cycling, a modality that uses functional electrical stimulation to produce cyclic pedalling through the coordinated activation of lower-limb muscles. In addition to enabling physical exercise for individuals with motor impairment, FES-Cycling offers advantages associated with mechanical movement stability, low joint impact, and the possibility of instrumenting and monitoring the system during the activity (Hunt *et al.*, 2012; Peng *et al.*, 2011).

Despite its potential, FES-Cycling presents important technical challenges. Artificially induced contraction differs from natural physiological recruitment because it tends to activate motor units more synchronously and less selectively, thereby increasing susceptibility to neuromuscular fatigue. In addition, the response to stimulation may vary between users and over time as a function of factors such as electrode placement, electrode–tissue interface impedance, muscle condition and training-related adaptations.

Another important aspect is that the mechanical contribution of each muscle group varies throughout the pedalling cycle. Stimulation applied outside mechanically favourable angular regions may produce reduced or zero torque, or even torque in the direction opposite to the desired crank rotation (Bellman *et al.*, 2016; Cousin *et al.*, 2020). Synchronisation between crank angular position and muscle-group activation is therefore a fundamental requirement for the performance of FES-Cycling systems.

In this setting, the development of instrumented platforms capable of monitoring movement, synchronising functional electrical stimulation and recording experimental data in a structured manner is relevant to the investigation of stimulation-parameter control and personalisation strategies. FES-Cycling therefore represents not only an application of FES in rehabilitation but also a multidisciplinary problem involving embedded electronics, sensing, signal processing, control and computational data analysis.

1.2 MOTIVATION

Conventional FES-Cycling systems often use stimulation angular ranges defined through empirical adjustments, anatomical references or values previously reported in the literature. Although this approach is simple to implement, it may not adequately represent individual user characteristics, the biomechanical properties of the system or changes arising from muscle fatigue over time.

In recent years, various approaches have been proposed to support the individualisation of stimulation parameters, including the use of torque sensors, musculoskeletal models, adaptive algorithms and computational techniques for analysing pedalling performance. These initiatives reflect a shift from strategies based predominantly on empirical adjustments towards approaches grounded in experimental data and quantitative evaluation criteria.

However, many of these solutions depend on additional mechanical instrumentation, complex biomechanical models or computational methods that are difficult to implement. There is therefore still a need for experimental platforms capable of monitoring crank angular position, synchronising functional electrical stimulation with the pedalling cycle and recording data in a structured manner, thereby enabling objective analysis of system performance.

The motivation for this thesis is based on the development and evaluation of an inertial-sensing FES-Cycling platform capable of integrating data acquisition, angular synchronisation and multichannel functional electrical stimulation. In addition, the study investigates strategies to support the definition and personalisation of stimulation angular ranges based on information obtained during experimental trials.

1.3 RESEARCH PROBLEM

The effectiveness of FES-Cycling systems depends directly on the appropriate definition of functional electrical stimulation parameters, particularly the stimulation angular ranges of the muscle groups involved in pedalling. Although various activation strategies have been proposed in the literature, these ranges are still often determined using pre-established protocols or empirical adjustments that may not adequately represent individual user characteristics.

In this context, it is relevant to investigate how pedalling kinematic information can be used to support the identification and personalisation of stimulation angular ranges, thereby contributing to the adaptation of FES parameters to the specific needs of each individual.

Accordingly, the research problem addressed in this thesis is the use of pedalling kinematic information to support the identification and personalisation of stimulation angular ranges in FES-Cycling systems.

1.4 PROPOSED APPROACH

To contribute to the development of FES-Cycling systems controlled according to crank angular position, this thesis proposes a platform capable of synchronising multichannel functional electrical stimulation using information obtained from an inertial sensor coupled to the bicycle's mechanical system.

The platform integrates data-acquisition, processing and storage modules, enabling the synchronised recording of pedalling kinematic variables and the stimulation parameters used during the experimental trials. This structure enables system performance to be evaluated under different stimulation configurations and allows the relationship between pedalling kinematics and the applied parameters to be analysed.

The data obtained are subsequently used to investigate computational strategies for supporting the definition and personalisation of functional electrical stimulation parameters, contributing to the development of FES-Cycling systems based on kinematic feedback.

The scope of this research is limited to the development and experimental evaluation of an inertial-sensing FES-Cycling platform and to the investigation of strategies for supporting the definition and personalisation of stimulation angular ranges. Long-term clinical rehabilitation, physiological adaptations resulting from continued FES use and the implementation of real-time adaptive-control systems are outside the scope of this thesis.

1.5 OBJECTIVES

1.5.1 General objective

To design, implement and experimentally evaluate an FES-Cycling system based on crank angular position, using inertial sensing to synchronise multichannel functional electrical stimulation (FES), and, as a complementary objective, to apply artificial-intelligence techniques based on artificial neural networks to support the estimation and personalisation of stimulation angular ranges using kinematic data obtained during the experimental trials.

1.5.2 Specific objectives

i. Implement an embedded electronic platform to acquire crank angular position and synchronise the application of functional electrical stimulation with movement.

ii. Develop a computational framework to acquire, organise, synchronise and process experimental data by integrating kinematic information and stimulation parameters.

iii. Establish quantitative indicators for evaluating and comparing the performance of different functional electrical stimulation configurations.

iv. Apply a Multilayer Perceptron (MLP) neural network in offline mode as a tool to support the estimation and personalisation of stimulation angular ranges.

v. Experimentally evaluate the performance of the platform and analyse the stimulation angular ranges suggested by the neural network using the kinematic indicators obtained from the trials.

1.6 CONTRIBUTIONS OF THE STUDY

The main contributions of this thesis are related to the development of an experimental FES-Cycling platform that integrates inertial sensing, multichannel functional electrical stimulation and structured data acquisition. The platform synchronises the application of FES with crank angular position, records and compares different stimulation configurations using kinematic indicators and, as a complementary component, uses an artificial neural network in offline mode to support the personalisation of stimulation angular ranges. Through this integration, the study combines instrumentation, data processing and computational support for analysing and adjusting stimulation configurations in FES-Cycling systems within a single framework.

1.7 THESIS STRUCTURE

Chapter 1 presents the background, motivation, research problem, proposed approach, objectives and contributions of the study.

Chapter 2 presents the foundations of FES-Cycling and related work, focusing on functional electrical stimulation, electrical parameters, pedalling biomechanics, angular synchronisation, sensing, control and stimulation-range personalisation.

Chapter 3 presents the materials and methods of the experimental platform. It details the electronic architecture, embedded subsystems, functional electrical stimulation (FES) stage and experimental methodology, as well as data processing and the computational approach based on an MLP artificial neural network.

Chapter 4 presents the experimental results and discussion, considering system performance under different stimulation configurations and the analysis of the proposed personalisation strategies.

Finally, Chapter 5 presents the general conclusions, the main contributions of the research, the study limitations and prospects for future work.

2 THEORETICAL FOUNDATIONS

This chapter presents the foundations of FES-Cycling from an analytical perspective oriented towards systems engineering and control. Although functional electrical stimulation involves clinical and neurophysiological variables, this review focuses on the development of instrumented systems. The critical design elements considered are the electrical parametrisation of the balanced biphasic stimulus, ion-transfer dynamics at the electrode–tissue interface, pedalling biomechanics and cycle asymmetries, angular-synchronisation strategies under electromechanical delay, and sensing and control loops for personalising stimulation angular ranges.

Accordingly, physiological phenomena are considered strictly as design requirements, operational constraints or sources of uncertainty–such as progressive fatigue and temporal variability–for data acquisition and control. The central aim is to consolidate the technical basis underlying the hardware and software architecture proposed in this thesis, characterised by the integration of multichannel stimulation, deterministic kinematic sensing of the crank, real-time signal processing and computational support for optimising muscle-switching profiles.

2.1 FES APPLIED TO NEUROMOTOR REHABILITATION

FES is a technique based on applying electrical pulses to excitable tissues in order to induce muscle contractions and assist in the recovery or partial substitution of impaired motor functions. It is used when voluntary motor control is reduced or when neural pathways cannot adequately activate peripheral muscles, as occurs in neurological conditions including spinal cord injury (SCI) and stroke (Peckham and Knutson, 2005; Lynch and Popovic, 2008).

In SCI, communication pathways between the central nervous system (CNS) and body segments below the injury level are partially or completely interrupted. Although the muscles may remain electrically excitable, voluntary motor commands become insufficient to produce functional movement. In this context, FES acts as an artificial neuromuscular activation pathway by stimulating intact peripheral motor nerves to produce task-oriented contractions (Peckham and Knutson, 2005; Lynch and Popovic, 2008).

From a neurophysiological perspective, FES applies trains of electrical pulses through electrodes positioned over regions close to motor nerves or muscle motor points. This thesis considers transcutaneous stimulation using surface electrodes. When the stimulus exceeds the tissue excitability threshold, the neural membrane depolarises and artificial action potentials are generated, initiating muscle contraction (Peckham and

Knutson, 2005; Maffiuletti, 2010).

FES-induced contraction differs substantially from physiological control. During voluntary movement, the CNS recruits motor units gradually, asynchronously and selectively, beginning with smaller, more fatigue-resistant units and incorporating larger units as force demand increases. With FES, recruitment tends to be more synchronous, spatially restricted and less selective. Consequently, larger fibres that are more susceptible to fatigue may be activated early, resulting in a less efficient response from metabolic and mechanical perspectives (Hunt *et al.*, 2012; Maffiuletti, 2010).

This non-physiological recruitment accelerates muscle fatigue, which is one of the main limitations of the technique. Repeated activation of the same motor units reduces the natural alternation between active and resting fibres. In functional applications, this fatigue compromises torque maintenance, reduces task-execution time and requires dynamic adjustment of stimulation parameters (Hunt *et al.*, 2012; Cousin *et al.*, 2020).

The response to FES depends on biological and instrumentation-related factors, including adipose-tissue thickness, electrode–skin interface impedance, electrode placement and the definition of electrical parameters such as current amplitude, pulse width and frequency. These parameters should be adjusted to generate functional torque, reduce discomfort and delay the onset of neuromuscular fatigue as far as possible (Lynch and Popovic, 2008; Coelho-Magalhães *et al.*, 2022).

FES-based systems can be regarded as dynamic systems subject to uncertainty, delays, nonlinearities and temporal variability. The force generated by the same stimulation pattern may change over time as a result of fatigue, neuromuscular adaptation and changes at the electrode–skin interface. Functional applications therefore require feedback loops and control strategies capable of adjusting stimulation based on the observed motor response (Bellman *et al.*, 2016; Cousin *et al.*, 2020).

Functional electrical stimulation-assisted cycling (FES-Cycling) applies this principle by coordinating stimulation of lower-limb muscle groups–particularly the quadriceps, hamstrings and gluteal muscles–to produce cyclic pedalling. The muscles are activated within specific portions of the cycle according to crank angular position (Bó *et al.*, 2017; Hunt *et al.*, 2012). System efficiency therefore depends on synchronisation among the electrical stimulus, crank kinematics and the user's biomechanical response.

2.2 STIMULATION PARAMETERS AND THE ELECTRODE–TISSUE INTERFACE

The muscle response induced by functional electrical stimulation (FES) depends on how the electrical parameters are applied to excitable tissue. The main parameters include current amplitude, pulse width and stimulation frequency. These elements determine the charge delivered to the tissue, the number of recruited motor units and the intensity of the resulting contraction (Peckham and Knutson, 2005; Maffiuletti, 2010).

Current amplitude controls the intensity of the electric field in the tissue. As current increases, a larger number of motor axons may reach the depolarisation threshold, increasing the generated muscle force. Pulse width defines the duration of current application in each stimulus phase; therefore, for the same amplitude, longer pulses inject more electrical charge and may recruit a greater volume of excitable tissue (Maffiuletti, 2010; Coelho-Magalhães *et al.*, 2022).

Stimulation frequency regulates the temporal summation of contractions. Low frequencies produce isolated or unfused contractions, whereas higher frequencies promote the tetanic fusion required for functional movement. However, increasing the frequency reduces the recovery interval of stimulated fibres and accelerates muscle fatigue. The choice of frequency therefore involves a trade-off among movement smoothness, torque production and fatigue mitigation (Maffiuletti, 2010; Hunt *et al.*, 2012).

In addition to amplitude and pulse width, stimulation frequency directly modulates the contractile dynamics of the stimulated muscle. Investigations based on mechanomyographic (MMG) responses during submaximal contractions indicate that changes in stimulation frequency and pattern can alter the observable mechanical response of muscle tissue (Papcke *et al.*, 2018). This perspective is relevant to *FES-Cycling* systems because it reinforces that electrical parameters should be evaluated not only according to the charge delivered to the tissue but also according to the kinematic and mechanical response induced during the functional task.

Table 1 summarises the function of the main electrical parameters used in FES and their functional effects. This synthesis shows that amplitude, pulse width and frequency do not act independently; together, these parameters determine neuromuscular recruitment, the force produced and the rate at which fatigue develops.

In addition to the parameters summarised in Table 1, the waveform is critical to stimulation safety. In transcutaneous stimulation, monophasic signals may cause a net accumulation of charge at the electrode–tissue interface, promoting electrochemical reactions, skin irritation and discomfort. For this reason, FES systems preferentially use balanced biphasic pulses, in which the charge injected during one phase is compensated by the subsequent phase of opposite polarity (Peckham and Knutson, 2005; Lynch and Popovic, 2008; Coelho-Magalhães *et al.*, 2022).

Figure 1 presents a representation of a balanced biphasic waveform. It identifies the electrical elements most relevant to stimulation: amplitude, phase duration, inter-phase interval and pulse period.

Amplitude defines the applied current level, phase duration determines the duration of each polarity phase, and the inter-phase interval separates the positive and negative

Table 1 – Main electrical parameters used in FES and their functional effects.

Parameter	**Main function**	**Functional effect**
Current amplitude	Defines the intensity of the stimulus applied to the tissue and contributes to the delivered electrical charge together with pulse width.	Increasing it tends to expand the spatial recruitment of motor units and increase the force or torque produced. However, high amplitudes may increase discomfort, reduce the selectivity of surface stimulation and accelerate fatigue, depending on electrode–tissue impedance, electrode placement and the individual's neuromuscular condition.
Pulse width	Defines the duration of each phase of the stimulation pulse and directly affects the electrical charge injected into the tissue.	Increasing pulse width may increase muscle recruitment and the mechanical response once the activation threshold is reached. However, longer pulse widths also increase the delivered charge and may affect comfort, tolerability and fatigue. Their effect depends on the applied amplitude, stimulated muscle, electrode–tissue interface and neuromuscular state.
Stimulation frequency	Defines the repetition rate of electrical pulses and controls the temporal summation of contractile responses.	Low frequencies tend to produce pulsatile contractions, whereas sufficiently high frequencies promote greater contraction fusion and smoother movement. However, high frequencies increase metabolic demand and may accelerate muscle fatigue. The choice therefore involves a trade-off among contraction smoothness, torque produced and the functional duration of the session.

Source: Based on (Peckham and Knutson, 2005; Lynch and Popovic, 2008; Maffiuletti, 2010; Hunt *et al.*, 2012).

phases of the same biphasic pulse. The pulse period determines the effective stimulation frequency. Charge balancing between the phases reduces residual polarisation at the electrode–skin interface and enables safer application of pulse trains during prolonged sessions.

From an electronic perspective, safe and reproducible pulse generation depends directly on the stimulator output stage. Power-amplifier circuits used in functional electrical stimulation systems must be designed to deliver pulses to biological tissue with amplitude, waveform and stability compatible with the therapeutic application (Souza *et al.*, 2017). In multichannel *FES-Cycling* systems, this stability is particularly important because repeatability of the applied current contributes to stimulus consistency across trials, enables controlled comparison of different stimulation configurations and strengthens experimental traceability.

Electrical coupling between the stimulator and biological tissue occurs at the electrode–tissue interface. In the circuit's metallic conductors, current is predominantly electronic; in biological tissue, conduction occurs through ions. The electrode therefore acts

Figure 1 – Representation of a balanced biphasic waveform used in functional electrical stimulation.

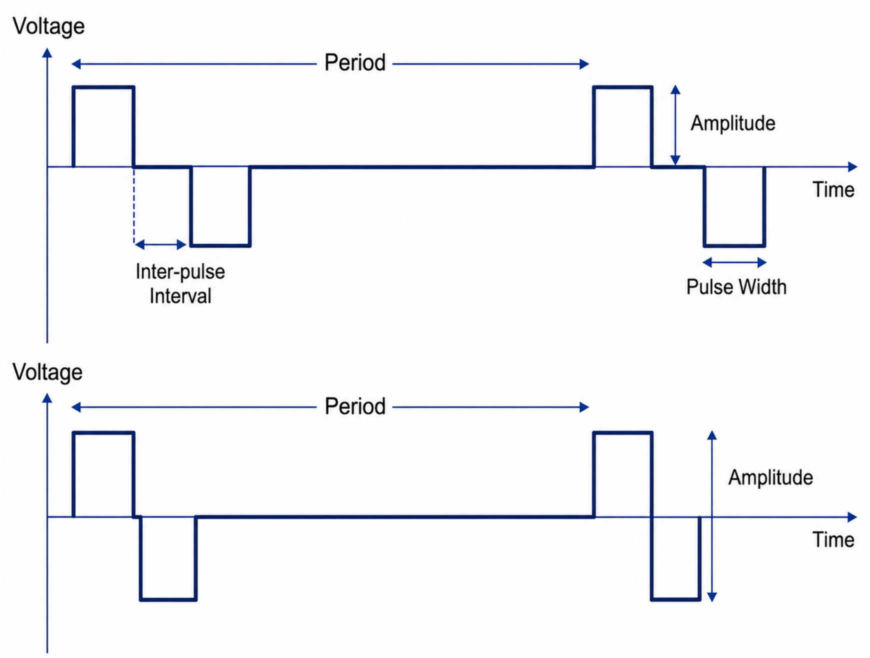

Source: Adapted from Peckham and Knutson (2005) and Lynch and Popovic (2008).

as a transducer between the electronic domain and the physiological medium. The efficiency of this transduction is limited by electrode–skin interface impedance, which varies with skin hydration, adipose-tissue thickness, contact area, mechanical pressure on the electrode and the conductivity of the coupling medium (Maffiuletti, 2010; Coelho-Magalhães *et al.*, 2022).

Electrode placement is also critical to the spatial selectivity of stimulation. Positioning electrodes over muscle motor points reduces the activation threshold and improves recruitment efficiency. Conversely, inadequate placement requires higher currents, increases discomfort, reduces energy efficiency and may induce co-activation of unintended muscles. In multichannel systems, this effect is particularly relevant because simultaneous activation of antagonistic muscles reduces the net torque available for the task (Maffiuletti, 2010; Sanna *et al.*, 2021).

In FES-Cycling, the parameters presented in Table 1 and the waveform shown in Figure 1 directly influence pedalling dynamics. Stimulation should produce sufficient torque to contribute to crank movement without unnecessarily increasing fatigue, discomfort or mechanically unfavourable activations. In addition, the torque response varies throughout a session because of muscle fatigue, temporal changes at the electrode–skin interface and the nonlinear dynamics of the stimulated muscle (Hunt *et al.*, 2012; Cousin *et al.*, 2020).

Consequently, the performance of FES-Cycling systems depends on appropriate control of electrical parameters and on the stability of the electrode–tissue interface. The platform proposed in this thesis addresses this requirement by integrating multichannel stimulation, kinematic acquisition and experimental recording, thereby relating the applied parameters, crank angular position and observed functional response. This integration is necessary to replace purely empirical protocols with stimulation strategies that are more controlled, repeatable and personalised.

2.3 INDEPENDENT MULTICHANNEL STIMULATORS

2.3.1 Need for stimulation channels with independent parameters

The application of *FES-Cycling* requires activation of different lower-limb muscle groups. Each muscle group contributes differently to crank movement and may require its own stimulation conditions. The stimulator must therefore have multiple output channels so that different muscles can be activated separately and in a coordinated manner.

The need for multiple channels is not limited to defining stimulation angular ranges. Each channel should allow individual adjustment of stimulation parameters, such as current amplitude, pulse width, frequency, pulse-train duration and activation timing. This independence is necessary because different muscles may have different activation thresholds, contractile responses and fatigue levels.

The multichannel architecture should be understood as a functional system requirement. It allows each channel to be associated with a specific muscle group, dedicated stimulation parameters to be defined and the activation sequence to be organised throughout the crank cycle.

This individualisation is also important because of variations in the electrode–skin interface, electrode placement, stimulated-muscle volume and progression of muscle fatigue. When different channels share the same parameters, some muscle groups may be understimulated while others may receive excessive stimulation. Channel independence and dedicated parameterisation therefore promote greater selectivity, improved control of the evoked motor response and better adaptation of the system to the dynamic demands of *FES-Cycling*.

2.3.2 Integration with sensors for closed-loop control

Closed-loop operation requires the stimulator to operate in integration with the processing unit and the system sensors. Variables measured during movement are used to define activation of the stimulation channels, replacing or complementing fixed temporal activation sequences.

In FES-Cycling systems, feedback may be obtained from sensors measuring position, velocity, force, torque or muscle activity. In this thesis, crank angular position is used as the feedback variable to synchronise FES-channel activation throughout the pedalling cycle. The processing unit continuously monitors instantaneous angular position and uses this information to determine whether each channel should be activated or deactivated according to the stimulation angular ranges previously defined for the corresponding muscle groups.

To enable this integration, the hardware architecture must support independent channel switching, maintain electrical-pulse timing and provide communication and processing latencies compatible with pedalling dynamics. The interface among the sensors, processing unit and stimulator is therefore a design requirement for closed-loop FES systems.

2.3.3 Limitations of commercial equipment and the need for dedicated platforms

Commercial electrical-stimulation equipment is widely used in conventional clinical and therapeutic applications. However, in research scenarios involving FES, closed-loop control and sensor integration, these devices may have limitations related to access to internal parameters, synchronisation with external systems and flexibility in modifying channel-activation logic.

In *FES-Cycling* applications, the stimulator must allow individual channel control, adjustment of electrical stimulation parameters, synchronisation with crank angular position and recording of the variables applied during trials. When commercial equipment imposes communication restrictions or does not provide suitable interfacing protocols, implementation of experimental control strategies may be limited.

For this reason, the literature frequently reports the use of dedicated, adapted or application-specific stimulators. These platforms provide greater control over the power stage, pulse timing, communication with sensors and embedded implementation of control algorithms. In the context of this thesis, this approach is appropriate because the proposed architecture depends on coordination between crank angular position and independent activation of the stimulation channels.

2.3.4 Multichannel-stimulator architectures reported in the literature

Stimulators used for FES are structured around two main blocks: a control stage and a power stage. The control stage defines the temporal stimulation parameters, manages active channels and, in feedback systems, processes signals from sensors. The power stage converts logic commands into electrical pulses applied to the electrodes while respecting the waveform, current range and electrical limits of the application (Junqueira, 2013; Rodríguez, 2016; Souza *et al.*, 2017).

In the studies reviewed, early microcontroller-based architectures already addressed electronic parameter adjustment, channel synchronisation and biphasic-pulse generation (Nohama, 1996; Casella, Bussador and Nohama, 1998; Bussador, Casella and Nohama, 1998). Portable systems with up to 16 channels and solutions with bidirectional telemetry for stimulator supervision were subsequently described (Faria, Carvalho and Nitatori, 2004; Faria and Carvalho, 2004). Stimulators were later integrated with acquisition and control modules for gait-generation applications in patients with spinal cord injury, including USB communication and movement monitoring in hemiplegic patients (Faria, 2006; Silva, Carvalho and Faria, 2006; Silva, 2007).

The incorporation of embedded controllers enabled automatic closed-loop strategies, such as PID controllers applied to functional neuromuscular stimulators (Prado, 2009). This development led to eight-channel microcontroller-based systems with rectangular biphasic waveforms, balanced charge and applications in lower-limb position control (Junqueira *et al.*, 2012; Junqueira, 2013; Junqueira *et al.*, 2013). Complete test platforms have also been proposed to integrate electrical stimulation, signal acquisition and lower-limb movement assessment (Sanches, 2013).

In the power stage, H-bridge architectures for generating biphasic pulses and controlled reversal of load-current direction are prominent (Gaiotto, 2012; Rodríguez, 2016; Rodríguez *et al.*, 2016). Current sources, current mirrors and voltage–current converters have also been used to control the current applied to tissue and reduce the influence of impedance variations at the electrode–skin interface (Rodríguez, 2016; Souza *et al.*, 2017; Gobbo, 2021). In addition, the power-supply stage has become a critical element in multichannel systems, requiring DC sources and DC–DC converters to adapt voltage levels to the power circuit (Souza, 2016).

In *FES-Cycling* applications, the electronic architecture must support independent channel activation, sensor integration and synchronisation of stimulation with crank angular position. The choice of system therefore depends on the number of channels, waveform, modulation strategy, current range, power-supply stage and ability to integrate with embedded control (Hernández, 2022; Coelho-Magalhães *et al.*, 2022).

2.4 BIOMECHANICS OF CYCLING APPLIED TO REHABILITATION

Cycling is a cyclic, repetitive and low-impact activity, characteristics that favour its use in neuromotor-rehabilitation protocols. Unlike gait, pedalling occurs along a mechanically constrained trajectory, reducing the demand for dynamic balance and allowing controlled repetition of lower-limb movement (Hunt *et al.*, 2012; Peng *et al.*, 2011). This condition is particularly relevant for individuals with spinal cord injury or other motor impairments, for whom assisted exercise may contribute to musculoskeletal, cardiovascular and metabolic maintenance (Peng *et al.*, 2011; Perkins *et al.*, 2002).

The mechanical configuration of the system directly influences the safety and clinical applicability of assisted pedalling. Upright bicycles or ergometers require greater postural control, whereas recumbent systems provide greater stability, trunk support and lower demand for voluntary balance. For this reason, recumbent platforms or adapted tricycles are frequently used in FES-Cycling applications for users with severe motor impairment (Sanna *et al.*, 2021; Coelho-Magalhães *et al.*, 2022).

The pedalling cycle can be described in terms of two main phases: the power phase and the recovery phase. During the power phase, the force applied to the pedal contributes predominantly to positive crank torque. During recovery, the limb returns to its initial position to allow the cyclic movement to continue. The effective contribution of each muscle depends on crank angular position, hip and knee joint angles and the direction of the resultant force applied to the pedal (Schutte *et al.*, 1993; Idsø, 2002).

Crank torque production is not uniform over 360°. Some regions of the cycle have lower-limb geometries that favour conversion of muscle force into propulsive torque, whereas this conversion is reduced in other regions. Near the top and bottom dead centres, the applied force tends to make a smaller tangential contribution to the crank, characterising regions of low mechanical effectiveness. In these intervals, inappropriate muscle activation may increase energy expenditure without making a substantial contribution to movement (Schutte *et al.*, 1993; Bellman *et al.*, 2016).

Pedalling involves coordinated action of lower-limb muscle groups. In FES-Cycling, the most relevant groups are the quadriceps, gluteal muscles and hamstrings because they are directly associated with knee extension, hip extension and knee flexion during the cycle. Table 2 summarises the biomechanical function of these groups and their relevance to functional electrical stimulation.

Table 2 – Main muscle groups involved in FES-assisted cycling.

Muscle group	**Main action**	**Contribution to the cycle**	**Relevance to FES-Cycling**
Quadriceps	Knee extension	Contributes mainly during the propulsive phase of pedalling.	Positive torque generation.
Gluteal muscles	Hip extension	Assists the power phase and movement stabilisation.	Propulsive support.
Hamstrings	Knee flexion and hip extension	Contribute to the transition between phases and limb recovery.	Cycle continuity.

Source: Prepared by the author.

Synchronisation between muscle activation and crank angular position is therefore a central biomechanical requirement. Stimulation applied outside the appropriate stimulation range may generate reduced or zero torque, or torque in the direction opposite to the desired movement. This condition is critical in FES-Cycling systems because muscle activation is not voluntarily commanded by the user but by an electronic system that must artificially coordinate the activation timing of each muscle group (Bellman *et al.*, 2016; Cousin *et al.*, 2020).

This principle justifies the use of sensors to measure crank angular position in real time. Rotary encoders, magnetic sensors or inertial measurement units can provide the kinematic variable required to identify the cycle phase and activate stimulation only in mechanically favourable regions (Sanna *et al.*, 2021; Coelho-Magalhães *et al.*, 2022). Pedalling biomechanics therefore provide the basis for defining stimulation angular ranges, which are discussed in the next section.

In the context of this thesis, biomechanical analysis of cycling supports the choice of an instrumented platform capable of relating crank angular position, stimulated muscle groups and the observed functional response. This integration is necessary to improve trial repeatability, reduce mechanically unfavourable activations and support personalisation of stimulation patterns in FES-Cycling.

2.5 STIMULATION RANGES IN FES-CYCLING

In FES-Cycling, electrical stimulation must be synchronised with crank angular position because the ability of each muscle group to generate positive torque varies throughout the rotation. Functional electrical stimulation (FES)-induced contraction does not automatically follow the user's motor intention; consequently, stimulation applied in a mechanically favourable region may contribute to propulsion, whereas the same stimulation applied elsewhere may produce reduced or resistive torque (Bellman *et al.*, 2016; Gföhler and Lugner, 2004). Crank angular position thus becomes the reference variable for coordinating the stimulation channels.

Stimulation angular ranges correspond to the portions of the pedalling cycle in which a muscle or muscle group is activated. For a muscle group m, the stimulation range may be represented as $F_m = [\theta_{i,m}, \theta_{f,m}]$, where $\theta_{i,m}$ and $\theta_{f,m}$ denote the initial and final activation angles, respectively. When a range crosses the angular origin, the activation logic must account for cycle continuity between 0° and 360° to avoid unintended interruptions in stimulation.

During the power phase, coordinated activation of the quadriceps and gluteal muscles promotes knee and hip extension, contributing to positive crank torque. During the recovery phase, the hamstrings assist knee flexion and limb transition to the next propulsive phase. This coordination reduces mechanically unfavourable activations and improves effort distribution throughout the cycle (Coelho-Magalhães *et al.*, 2022; Sanna *et* *al.*, 2021).

Stimulation outside the appropriate range directly compromises system performance. Early or delayed activation may reduce cadence, increase discomfort, accelerate fatigue and generate torque components opposite to the desired movement. This problem is aggravated by electromechanical delay, defined as the interval between application of the electrical pulse and effective development of muscle force. For a cadence n in revolutions per minute and a delay Δt in seconds, the approximate angular displacement is $\Delta\theta \approx 6n\Delta t$. Thus, at 60 rpm, a 100 ms delay corresponds to approximately 36° of crank rotation (Bellman *et al.*, 2017; Cousin *et al.*, 2020).

Fixed stimulation ranges are simple to implement and suitable for initial trials, but they do not necessarily represent the best condition for all users, cadences and mechanical configurations. Anthropometry, seating position, crank length, fatigue, injury level and individual neuromuscular response alter the timing at which each muscle produces useful torque. Personalised stimulation ranges are therefore more appropriate for experimental platforms because they allow stimulation to be adjusted to the observed functional response (Gföhler and Lugner, 2004; Guillou *et al.*, 2021).

Implementing stimulation angular ranges requires reliable measurement of crank position. Encoders provide a direct, high-resolution angle measurement; magnetic sensors may be used for angular reference, passage detection or redundancy; and inertial measurement units (IMUs) may estimate movement phase when reduced mechanical coupling to the shaft is desired or when multiple sensing sources are combined (Baptista, Sijobert and Coste, 2018; Guillou *et al.*, 2021).

Table 3 summarises examples of stimulation angular ranges reported for the right and left legs. The muscle groups directly related to the FES-Cycling system used in this thesis were considered: quadriceps (Q), hamstrings (H) and gluteal muscles (G). The values should be interpreted according to the angular convention adopted by each source because different studies may define the 0° point at different crank positions.

The stimulation angular duration of each muscle group was calculated from the angular ranges presented in Table 3. When a range crosses the angular origin, the calculation accounts for cycle continuity between 0° and 360°, namely, $\Delta\theta = (360° - \theta_i) + \theta_f$. When the range does not cross the origin, $\Delta\theta = \theta_f - \theta_i$ is used. The results are presented in Table 4.

The comparison presented in Table 3 shows that stimulation angular ranges are not uniform across studies and may differ between the right and left sides. In addition, Table 4 shows that stimulation angular duration also varies considerably between protocols, even

Table 3 – Stimulation angular ranges for the quadriceps (Q), hamstrings (H) and gluteal muscles (G) in the right and left legs.

Source	Limb	Q start	Q end	H start	H end	G start	G end
(Peng *et al.*, 2011)	Right	0°	70°	28°	120°		
	Left	208°	300°	170°	250°		
(Hunt *et al.*, 2012)	Right	125°	20°	350°	272°	90°	0°
	Left	305°	205°	170°	92°	270°	180°
(Sousa *et al.*, 2016)	Right	300°	40°	70°	170°	30°	100°
	Left	120°	325°	290°	340°	240°	250°
(Schmoll *et al.*, 2022)	Right	72°	255°	181°	351°		
	Left	259°	68°	29°	184°		

Source: Prepared by the author. Empty cells indicate that the range was not reported in the consulted source.

Table 4 – Stimulation angular duration for the quadriceps (Q), hamstrings (H) and gluteal muscles in the right and left legs.

Source	Limb	Quadriceps (Q)	Hamstrings (H)	Gluteal muscles (G)
(Peng *et al.*, 2011)	Right	70°	92°	
	Left	92°	80°	
(Hunt *et al.*, 2012)	Right	255°	282°	270°
	Left	260°	282°	270°
(Sousa *et al.*, 2016)	Right	100°	100°	70°
	Left	205°	50°	10°
(Schmoll *et al.*, 2022)	Right	183°	170°	
	Left	169°	155°	

Source: Prepared by the author based on the angular ranges reported in Table 3.

for the same muscle group. This variability reflects differences in the adopted angular reference, system geometry, selected muscle groups, evaluated population and control strategy.

These differences reinforce the need for instrumented platforms capable of recording crank angular position, comparing protocols and supporting personalisation of stimulation angular ranges. In the context of this thesis, personalising these ranges is essential to increase the contribution of positive torque, reduce mechanically unfavourable activations and improve the repeatability of FES-Cycling trials.

2.6 INSTRUMENTATION AND CONTROL IN FES-CYCLING

The performance of FES-Cycling systems depends on the ability to measure the state of the pedalling cycle and adjust stimulation according to the user's response. Unlike voluntary movement, in which the central nervous system integrates sensory information and continuously corrects muscle action, FES-Cycling requires electronic instrumentation to coordinate muscle activation artificially with crank kinematics (Bellman *et al.*, 2017; Cousin *et al.*, 2020).

The variables most relevant to this process include crank angle, cadence, angular velocity, force or torque applied to the pedal and stimulation current. Crank angle is the primary variable for defining stimulation angular ranges, whereas cadence enables assessment of movement regularity. Force or torque measurements provide direct information about the user's mechanical contribution, and current monitoring contributes to trial safety and repeatability (Sanna *et al.*, 2021; Coelho-Magalhães *et al.*, 2022).

Sensor selection depends on the variable of interest and the platform architecture. Optical or magnetic encoders are frequently used to measure crank angular position with high resolution. IMUs can estimate orientation, angular velocity and phase events with less dependence on rigid mechanical coupling. Magnetic sensors may be used for simple detection of angular events, whereas load cells and current sensors enable assessment of the system's mechanical and electrical responses, respectively (Baptista, Sijobert and Coste, 2018; Guillou *et al.*, 2021; Sanna *et al.*, 2021).

Table 5 – Sensors applicable to monitoring FES-Cycling systems.

Sensor	**Measured variable**	**Advantage**	**Limitation**
Encoder	Crank angle and cadence	High resolution and direct measurement of angular position	Requires mechanical coupling to the shaft or crank
IMU	Orientation, angular velocity and phase events	Flexible installation and measurement of moving segments	Susceptible to drift and noise and requires calibration
Magnetic sensor	Discrete angular events	Simple, low-cost and operationally robust	Limited angular resolution
Load cell	Force or torque applied to the pedal	Direct measurement of mechanical contribution	Greater mechanical and electronic complexity
Current sensor	Stimulation current	Monitoring of stimulation safety and repeatability	Measures the electrical input, not the mechanical response

Source: Prepared by the author.

From a control perspective, FES-Cycling systems can be classified as open-loop or closed-loop. In open-loop systems, stimulation parameters and angular ranges are defined in advance and applied without automatic correction based on the user's response. This approach is simple but has important limitations because it does not compensate for muscle fatigue, changes at the electrode–skin interface, cadence variations or biomechanical differences between individuals (Hunt *et al.*, 2012; Bellman *et al.*, 2017).

In closed-loop systems, sensors provide information about system state and the controller adjusts stimulation to reduce the error between the measured response and a desired reference. Controlled variables may include cadence, torque, power or angular position. The control input may be modified through current amplitude, pulse width, frequency or a combination of these parameters. This structure allows disturbances and temporal variations in the muscular response to be compensated for, although it remains limited by stimulus saturation, electromechanical delay and progressive fatigue (Cousin *et al.*, 2019; Cousin *et al.*, 2020; Duenas *et al.*, 2020).

Personalisation of stimulation angular ranges is another central requirement. The position at which a muscle contributes positively to crank torque depends on anthropometry, seating position, crank length, injury level and the user's neuromuscular condition. Fixed stimulation ranges may therefore serve as an initial reference, but they do not necessarily represent the best configuration for all users or experimental conditions (Gföhler and Lugner, 2004; Wannawas and Faisal, 2023).

Computational methods can support this personalisation by reducing dependence on empirical adjustments. Biomechanical models, optimisation algorithms and artificial-intelligence techniques can be used to estimate more appropriate stimulation ranges while considering the observed kinematic and mechanical response. In this thesis, this concept is treated as support for personalisation and does not replace the need for reliable instrumentation and experimental validation (Farhoud and Erfanian, 2014; Wannawas and Faisal, 2023).

Table 6 summarises the main strategies reported in the literature and their implications for instrumented FES-Cycling systems.

Table 6 – Control strategies applied to FES-Cycling.

Strategy	**Principle**	**Advantage**	**Limitation**
Open loop	Applies predefined stimulation angular ranges and electrical parameters.	Simple implementation and low computational cost.	Does not compensate for fatigue, disturbances or individual variations.
Closed loop	Adjusts stimulation based on the error between the measured variable and the desired reference.	Compensates for cadence, torque or power variations during the task.	Depends on reliable sensors and may be limited by electromechanical delay.
PID control	Modulates the stimulation input using proportional, integral and derivative terms.	Simple structure widely used for cadence control.	May lose performance during rapid movements because of delays and muscle nonlinearities.
Fuzzy control	Uses linguistic rules to adjust stimulation according to the error and observed response.	Handles uncertainty without requiring a precise mathematical model.	Requires empirical rule definition and careful parameter tuning.
Hybrid control	Combines feedforward action and feedback to improve dynamic response.	Combines rapid response with disturbance compensation.	May require initial calibration, system identification or controller learning.
Intelligent control	Uses neural networks, reinforcement learning or optimisation to estimate parameters or stimulation ranges.	Promotes personalisation and interindividual adaptation.	Requires sufficient experimental data and rigorous validation.

Source: Prepared by the author based on Farhoud and Erfanian (2014), Bellman *et al.* (2017), Cousin *et al.* (2019), Cousin *et al.* (2020), Duenas *et al.* (2020) and Wannawas and Faisal (2023).

Control strategies applied to FES-Cycling differ in terms of the monitored variable, the adjusted stimulation parameter and the ability to compensate for disturbances. In simpler systems, stimulation may be applied in open loop using predefined parameters. In more advanced approaches, closed-loop control uses measurements such as cadence, torque, power or angular position to adjust stimulation according to the user's response.

The synthesis presented in Table 6 shows that no single strategy can address all the limitations of FES-Cycling. Open-loop methods are simple but have limited adaptability. Closed-loop strategies improve cadence stability and can compensate for disturbances, but they depend on sensing quality and remain subject to muscle fatigue and electromechanical delay. Hybrid and intelligent strategies increase personalisation capability but require greater experimental and computational complexity.

The platform proposed in this thesis fits within this context by integrating kinematic acquisition, multichannel stimulation, experimental monitoring and support for personalising stimulation angular ranges. Crank angular position is used as the feedback variable to synchronise FES-channel activation throughout the pedalling cycle, while electrical stimulation parameters are predefined or adjusted manually during the trials. This integration relates stimulation configurations to the observed kinematic response and provides a more structured basis for conducting and comparing FES-Cycling trials.

2.7 STRATEGIES FOR CONTROLLING ELECTRICAL STIMULATION IN FES-CYCLING

Defining stimulation angular ranges is a critical step in FES-Cycling systems because it determines the regions of the cycle in which each muscle group is activated. Traditionally, these ranges may be defined using empirical patterns, anatomical references or manual adjustments made during user preparation. Although operationally simple, this approach depends on operator experience, requires successive adjustment attempts and may induce fatigue before the main trial even begins (Schmoll *et al.*, 2022; Wannawas and Faisal, 2023).

Recent literature has sought to reduce this empirical dependence through automatic or semi-automatic personalisation methods. These methodologies differ in the type of data used, the variable optimised and the point at which adaptation occurs. In general, the approaches can be grouped into three main categories: methods based on the muscle's mechanical contribution, methods for online adaptation of electrical parameters, and methods based on biomechanical models combined with computational learning.

Among the approaches directly related to defining stimulation angular ranges, the OIDA (*Optimal Interval Detection Algorithm*) proposed by Schmoll *et al.* (2022) is notable. This method is based on the principle that a muscle should be stimulated only in the regions of the cycle in which its contraction contributes positively to crank rotation. To identify these regions, passive cycles without electrical stimulation and active cycles with continuous stimulation of a specific muscle or muscle group are recorded.

Passive torque is the torque measured during pedalling cycles performed without electrical stimulation. It includes the effects of gravity, segmental inertia, mechanical friction, passive tissue properties and externally imposed limb movement. Active torque, in contrast, is measured during equivalent cycles with continuous stimulation. It therefore contains both the passive components of the system and the additional contribution generated by evoked contraction.

The effective mechanical contribution of the stimulated muscle is estimated using net torque, defined as the difference between active and passive torque throughout the pedalling cycle:

$$\tau_{\text{net}}(\theta) = \tau_{\text{active}}(\theta) - \tau_{\text{passive}}(\theta), \tag{1}$$

where θ represents crank angular position. When $\tau_{\text{net}}(\theta) > 0$, the muscle is considered to contribute to propulsion; when $\tau_{\text{net}}(\theta) < 0$, the contraction tends to resist movement. OIDA therefore determines stimulation angular ranges from the regions in which net torque is positive (Schmoll *et al.*, 2022).

In the study by Schmoll *et al.* (2022), the methodology was applied to an adapted FES-Cycling tricycle instrumented with a crank power meter and inertial measurement units on the thighs. The algorithm was evaluated in a participant with complete spinal cord injury, considering the quadriceps and hamstrings bilaterally. The ranges were determined both as a function of crank angle and from a normalised phase derived from thigh movement. The method identified muscle-specific ranges and enabled stable cycling for 5 minutes without further adaptation of the stimulation pattern.

Another line of research investigates adaptation of electrical parameters during the session itself. Coelho-Magalhães, Coste and Resende-Martins (2022) proposed a hybrid strategy in which a proportional–integral (PI) controller tracks a reference cadence while a reinforcement-learning (RL) agent modifies the amplitude and pulse width of the stimulation channels. In this approach, the angular ranges are retained as part of the baseline pattern, while the agent acts on the electrical parameters to adapt the injected charge to the dynamic muscular response.

The study by Coelho-Magalhães, Coste and Resende-Martins (2022) was conducted during outdoor cycling with a participant with complete spinal cord injury. The vastus medialis, vastus lateralis combined with the rectus femoris, and hamstrings were stimulated bilaterally. The system used a frequency of 35 Hz, a pulse width between 450 and 600 μs and a current limited to 100 mA. The results indicated that the PI controller combined with the RL agent could track the reference cadence and adapt the stimulation pattern throughout the session. Under greater mechanical demand, sessions with RL enabled achieved greater distances than sessions using PI control alone, suggesting potential for compensating for temporal changes in the muscular response.

A third approach combines musculoskeletal modelling and computational learning. Wannawas and Faisal (2023) proposed a two-stage method for learning stimulation patterns in FES-Cycling. First, a personalised OpenSim model is constructed from the user's geometry and the system's mechanical configuration. A reinforcement-learning agent is then trained in the model to find activation patterns associated with crank angle. In the second stage, the pattern obtained through simulation is refined using real cycling data by means of offline reinforcement learning.

In the experimental evaluation by Wannawas and Faisal (2023), the method was tested on a stationary tricycle with an able-bodied participant. Three patterns were compared: an electromyography (EMG)-based pattern, a model-derived pattern and a pattern fine-tuned using real data. With only 100 s of real data for fine-tuning, the refined pattern produced the highest mean pedalling speed, reaching 52.37 rpm, compared with 49.83 rpm for the model-based pattern and 48.13 rpm for the EMG-based pattern. These results indicate that experimental data can improve patterns initially estimated from a model, although validation was performed in an unimpaired participant.

Table 7 summarises the main characteristics of these methodologies. The comparison shows that recent approaches converge on the same general objective: reducing arbitrariness in the definition of stimulation patterns and increasing adaptation to the individual characteristics of the user and system.

Table 7 – Recent methodologies for stimulation personalisation in FES-Cycling.

Source	**Strategy**	**Data used**	**Main result**
Schmoll *et al.* (2022)	Automatic detection of stimulation angular ranges based on positive net torque.	Passive and active torque, crank angle and IMU-based normalised phase.	Bilateral identification of quadriceps and hamstring ranges, with stable cycling for 5 minutes without further adaptation.
Coelho-Magalhães, Coste and Resende-Martins (2022)	PI cadence control combined with online reinforcement learning to adjust amplitude and pulse width.	Crank angle, cadence, cadence error, current, pulse width and estimated electrical charge.	Cadence tracking and adaptation of stimulation parameters during outdoor cycling sessions.
Wannawas and Faisal (2023)	Reinforcement learning in a personalised musculoskeletal model followed by fine-tuning with real data.	OpenSim model, crank angle, cadence and real cycling data.	A pattern refined with 100 s of real data achieved a higher mean speed than the EMG-based and model-only patterns.

Source: Prepared by the author.

The synthesis presented in Table 7 shows that personalisation in FES-Cycling can be approached in different ways: direct measurement of mechanical contribution, online adaptation of electrical parameters, or learning patterns from models and real data. Despite their methodological differences, these studies reinforce the need for instrumented platforms capable of synchronously recording kinematic, electrical and functional variables. This basis is essential for transforming empirically defined stimulation patterns into procedures that are more reproducible, quantifiable and adaptable.

2.8 FES-CYCLING AS A CYBATHLON DISCIPLINE

CYBATHLON is an international assistive-technology competition, informally often described as a 'bionic Olympics', in which people with disabilities perform functional tasks with the assistance of robotic systems, prostheses, orthoses, neural interfaces and functional electrical stimulation. One of its disciplines is *FES-Cycling*, in which pedalling is produced through electrical activation of the lower-limb muscles. In the context of this thesis, its relevance lies not in the competitive aspect itself but in its use as an applied scenario for assessing the robustness, safety, performance and repeatability of FES systems under conditions close to real-world use.

In the 2024 edition, the FES-Cycling discipline took place in a virtual environment, with participants required to cover 1960 m in up to 8 min. This format required integration of a tricycle or adapted bicycle, a stimulation system, cadence or power sensors and smart training rollers. The event therefore provided a practical reference for evaluating FES-Cycling solutions not only in terms of movement generation but also in relation to cadence maintenance, power, fatigue resistance and system stability (Savona *et al.*, 2026; Schmoll *et al.*, 2026).

Studies associated with CYBATHLON 2024 show that instrumentation is critical to performance. Although smart trainers and instrumented pedals can standardise interaction with the virtual environment, power measurement at low intensities, which are frequently observed in individuals with complete spinal cord injury, may present substantial errors. This limitation reinforces the need for consistent data acquisition and caution when interpreting mechanical metrics while sensors operate near the lower limit of their useful range (Schmoll *et al.*, 2026).

From a control perspective, the reported systems predominantly use instrumented recumbent tricycles, angular-position sensors, multichannel stimulators and cadence-control strategies. The Polimi team, for example, used proportional–integral (PI) control to modulate stimulation current and experimentally optimised the angular ranges based on tangential-force measurements. This optimisation increased the time required for the controller to reach saturation by 99%, indicating that the choice of stimulation ranges directly influences the ability to maintain cadence under fatigue (Savona *et al.*, 2026).

In addition to experimental approaches, recent studies associated with CYBATHLON development have explored strategies based on musculoskeletal simulation. In this context, Peres *et al.* (2025) proposed an approach using OpenSim Moco and muscle synergies to generate individualised stimulation patterns. Although the refined empirical protocol still produced greater power and mean cadence, the simulation-derived pattern produced physiologically structured activation and improved inter-limb symmetry, suggesting potential for model-based personalisation.

Table 8 – Contributions of studies related to CYBATHLON 2024 to FES-Cycling systems.

Source	**System**	**Strategy analysed**	**Contribution to this thesis**
Savona *et al.* (2026)	Instrumented recumbent tricycle for FES-Cycling	PI cadence control and experimental optimisation of angular ranges based on tangential force	Shows that stimulation ranges affect controller saturation and cadence maintenance under fatigue.
Schmoll *et al.* (2026)	Virtual environment with a smart trainer and power pedals	Assessment of power-sensor accuracy at low intensity	Reinforces the need for consistent experimental acquisition and caution when interpreting power in FES-Cycling.
Peres *et al.* (2025)	OpenSim Moco musculoskeletal model applied to FES-Cycling	Pattern generation through predictive simulation and muscle synergies	Shows a model-based alternative for generating individualised stimulation patterns.
Sanna *et al.* (2025)	Instrumented recumbent tricycle in a longitudinal FES-Cycling programme	Assessment of functional and physiological effects after prolonged training	Demonstrates the importance of repeatable, instrumented protocols for quantifying performance and training adaptation.

Source: Prepared by the author.

Table 8 summarises recent contributions associated with CYBATHLON 2024 that are relevant to FES-Cycling systems. The purpose of the table is not to compare competitive performance with the trials in this thesis but to identify technological trends related to instrumentation, control, stimulation-range personalisation and functional-performance assessment.

The synthesis presented in Table 8 shows that CYBATHLON 2024 can be treated as an applied validation environment for FES-Cycling solutions. The studies associated with the event reinforce four requirements directly related to this thesis: reliable measurement of pedalling kinematics, personalisation of stimulation angular ranges, cadence control and critical assessment of low-power mechanical metrics. These aspects support the relevance of an instrumented and modular platform capable of recording trials, comparing stimulation patterns and supporting personalisation processes.

2.9 LITERATURE SYNTHESIS AND SCIENTIFIC GAP

The analysis of the studies shows that FES-Cycling can be characterised as a complex multivariable-control system whose performance depends on the interaction among electrical stimulation parameters, pedalling biomechanics, angular-position sensing and the appropriate definition of stimulation angular ranges. The studies analysed reveal recurring challenges associated with applying FES in assisted-cycling systems, including early muscle fatigue, low mechanical efficiency, interindividual variability, electromechanical delay and variations in electrode–tissue interface impedance. In addition, stimulation angular ranges are still often defined through empirical procedures based on observing user performance and relying on operator experience. Overall, the literature demonstrates significant progress in the development of FES-Cycling systems but shows that determining and adapting stimulation angular ranges remain important challenges, particularly given the variability of neuromuscular and biomechanical responses observed among individuals. These aspects reinforce the need for research aimed at understanding and improving the methods used to define stimulation parameters in FES-Cycling applications.

3 MATERIALS AND METHODS

3.1 ARCHITECTURE AND INSTRUMENTATION DEVELOPED FOR FES-CYCLING

3.1.1 General architecture of the proposed system

The system architecture coordinates the interaction among the user, the instrumented bicycle, the crank inertial module, the central control unit and the functional electrical-stimulation units. The structure adopts a modular organisation that separates acquisition, processing, communication, power supply, safety and electrical-stimulation functions, enabling individual tests, progressive integration and future expansion.

Figure 2 – Functional architecture of the electronic system proposed for FES-Cycling applications.

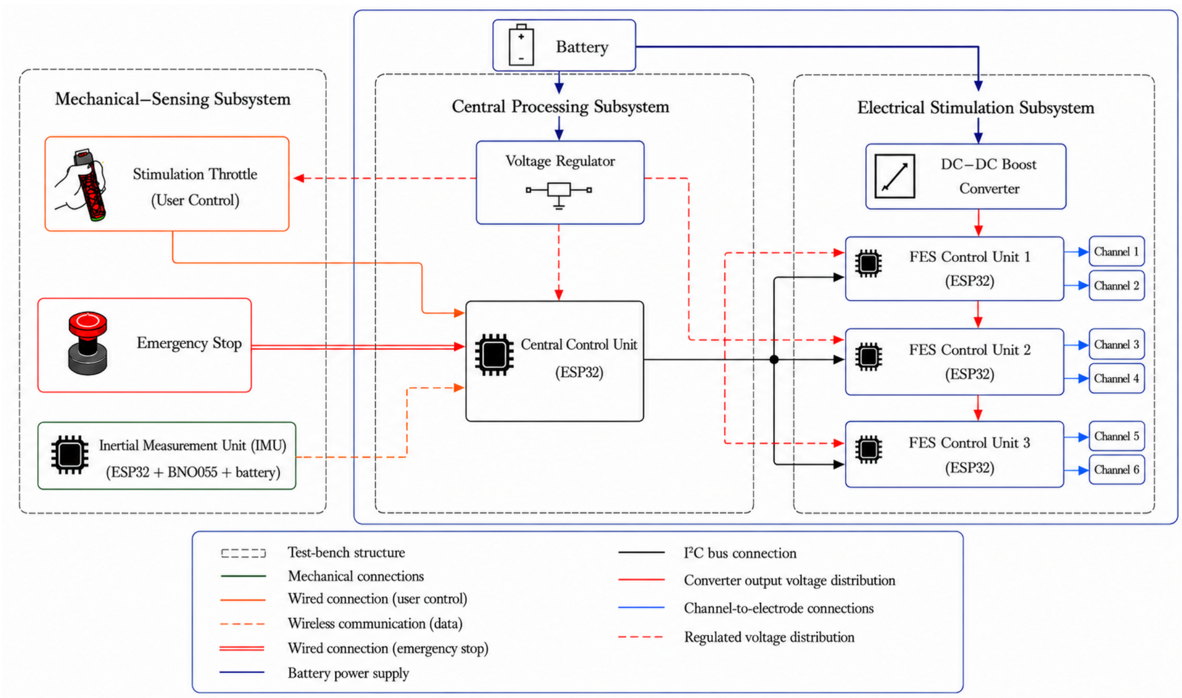

Source: Prepared by the author.

The functional architecture of the system is illustrated in Figure 2. The IMU, fixed to the crank arm, acquires angular kinematics and transmits the data to the central unit through Wi-Fi-based wireless communication. The central unit simultaneously processes the manual intensity-adjustment input and the emergency-stop device. From these variables, the algorithm generates commands for the FES units, which activate the stimulation channels according to the fixed angular ranges configured for the experimental protocol.

3.1.1.1 Functional architecture of angular-position feedback control

The implemented architecture places the FES-Cycling system in a kinematic closed-loop configuration in which crank angular position is used to switch the FES channels. The variable $\theta(t)$, estimated by the crank-mounted inertial module, is used by the central control unit to determine when the FES channels are activated and deactivated.

In this thesis, the system operates in closed loop with feedback of crank angular position. The position measured by the inertial sensor is continuously used by the central unit to identify the region of the pedalling cycle occupied by the crank and, on that basis, determine which FES channels should be activated according to the predefined stimulation ranges. Feedback is therefore used specifically to synchronise stimulation with crank movement. Current amplitude, in contrast, is not adjusted automatically by the loop; it is set in advance or modified manually during the trials.

The central unit continuously compares the instantaneous crank position with the stimulation range assigned to each muscle group. When the measured position lies within the range configured for a given channel, the corresponding FES unit is enabled; otherwise, the channel remains disabled. Stimulation is thus synchronised with the pedalling cycle, reducing dependence on sequences based solely on fixed timing.

Figure 3 presents the functional representation of the angular closed loop adopted in this thesis. The angular FES activation block receives the instantaneous crank position and the configured stimulation ranges, generating the commands sent to the FES units. Stimulation acts on the lower-limb muscles and contributes to movement of the crank–pedal assembly. As movement proceeds, angular position is estimated again by the inertial module and fed back to the central unit, enabling continuous updating of FES-channel activation and completing the feedback loop.

Figure 3 – Functional representation of the crank-position-based closed loop used to synchronise the FES channels in the FES-Cycling system.

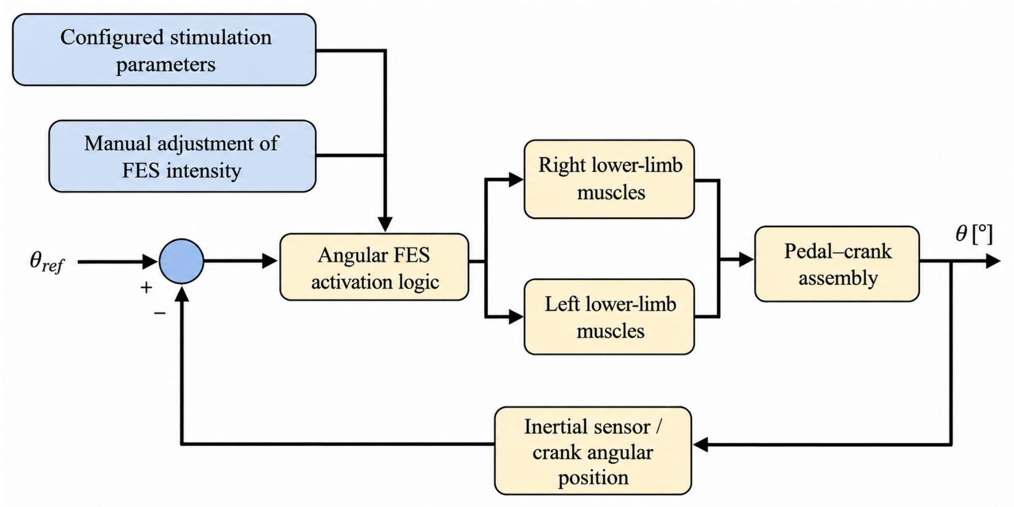

Source: Prepared by the author.

In addition to angular activation, the architecture provides structured experimental-data logging. Time, angular position, stimulation ranges and trial parameters are stored for subsequent processing, comparison between configurations and support for personalisation of angular ranges. The detailed mathematical formulation of the activation logic, including treatment of ranges crossing the transition between 360° and 0°, is presented in Section 3.1.3.

3.1.1.2 Physical integration of the modules in the experimental platform

The mechanical platform is based on a *recumbent tricycle* selected for its structural stability, postural support and ergonomic suitability for mounting the electronic modules. The recumbent configuration reduces the user's need for dynamic balance and facilitates spatial distribution of the components: the IMU is mounted on the crank, the manual controls remain within reach and the FES units occupy the rear region of the chassis.

This mechanical configuration was maintained throughout the trials to preserve comparable conditions across the experimental stages. The *trike* was adjusted to provide suitable participant positioning and unrestricted lower-limb movement during pedalling, without changing the arrangement of the embedded modules or controls.

The power-management system was organised into functional voltage levels. The main battery supplies the platform, while its voltage is stepped down and regulated for the control, sensing and communication circuits. In parallel, a *boost* DC–DC converter raises the battery voltage to the level required by the electrical-stimulation power stage. This topology functionally separates the low-power paths associated with control and communication from the higher-power paths associated with functional electrical stimulation.

Figure 4 – Physical integration of the main electronic modules in the *tricycle*-based FES-Cycling platform.

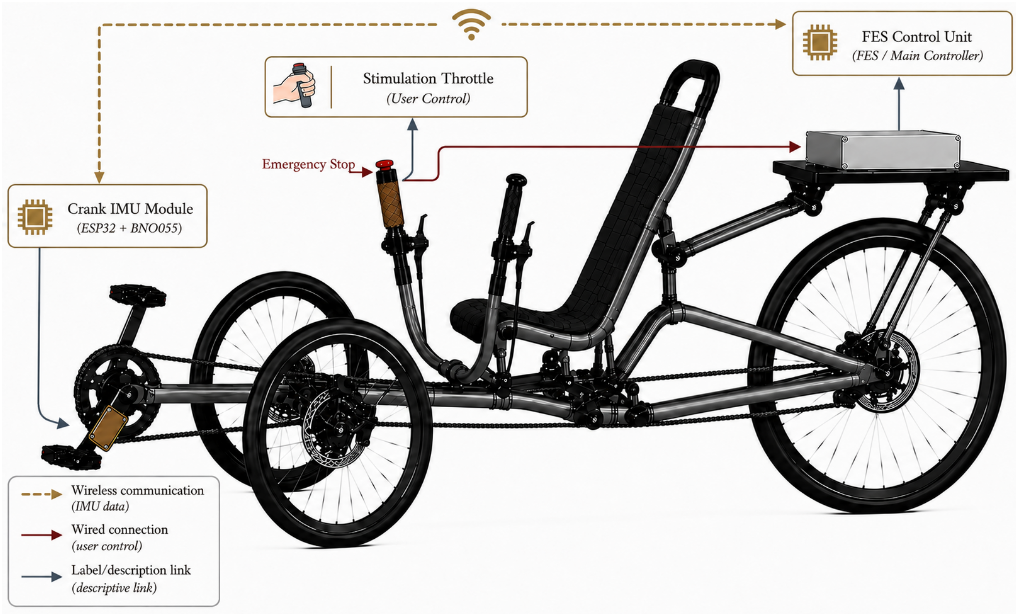

Source: Prepared by the author.

The physical arrangement and coupling of the modules are shown in Figure 4, demonstrating the direct correspondence between the functional diagram and the physical assembly: crank-mounted IMU, stimulation control, emergency button, central control unit and FES modules.

3.1.2 Embedded electronic subsystems

The embedded electronic subsystems were organised according to their platform functions: central processing, sensing, manual interface, electrical stimulation and power supply. This division supports a modular description of the architecture while preserving functional separation between the control, communication, operational-safety and FES-activation blocks. Table 9 summarises the main implemented modules.

3.1.2.1 Central control unit

The central control unit is the logical core of the platform. It receives commands from the manual interface, monitors the emergency-stop state, interprets data transmitted by the crank IMU module and coordinates commands sent to the FES units. The ESP32 integrates embedded processing and wireless communication in a compact platform suited to the physical distribution of the modules on the bicycle.

Within the proposed architecture, the central unit executes the angular-switching logic of the FES channels. The crank angular position received from the IMU module is

Table 9 – Main embedded electronic subsystems in the FES-Cycling platform.

Subsystem	**Main components**	**System function**
Central control unit	ESP32, control inputs and communication interface	Process signals, coordinate overall operation and send commands to the FES units.
Crank IMU module	ESP32, BNO055 and dedicated battery	Measure crank angular movement and transmit the data through Wi-Fi.
Manual interface	Stimulation control and emergency stop	Permit manual intensity adjustment and rapid system interruption.
FES units	Three ESP32-based units, with two channels per unit	Activate six independent stimulation channels.
Electrical-stimulation stage	H-bridge, current-control circuit and electrode output	Generate biphasic rectangular pulses with current control.
Electrical supply	Battery, voltage regulator and *boost* DC–DC converter	Provide the voltage levels required by the logic circuits and FES stage.

Source: Prepared by the author.

compared with the fixed ranges configured for each muscle group. When the measured position belongs to the corresponding range, the associated FES channel is enabled; otherwise, it remains disabled.

3.1.2.2 Crank inertial module

The crank inertial module was developed to provide the principal kinematic variable of the FES-Cycling platform: instantaneous crank angular position. The central control unit uses this variable to execute the angular-switching logic of the FES channels according to the fixed ranges configured for each muscle group.

Installing the inertial sensor directly on the crank arm associates the measured orientation with the mechanical pedalling cycle. The angular estimate provided by the IMU module therefore supplies a geometric reference for identifying the instantaneous phase of movement and synchronising stimulation-channel activation.

The choice of an inertial measurement unit rather than an encoder mechanically coupled to the crank axle was motivated by instrumental simplicity, portability and reduced structural interference with the bicycle. The IMU avoids extensive machining, precise mechanical alignment and invasive modification of the bottom bracket, facilitating installation on different recumbent-bicycle or *trike* geometries.

The sensor used was the BNO055, which integrates an accelerometer, gyroscope and magnetometer in a single device. Its embedded sensor-fusion processing estimates module orientation without relying exclusively on temporal gyroscope integration. This feature helps reduce angular drift and provides a more stable estimate of crank position during the trials.

The module comprises an ESP32, a BNO055 sensor and a dedicated battery. Wi-Fi-based wireless communication avoids cabling in a region subject to continuous rotation, reducing mechanical constraints and simplifying experimental assembly. In this thesis, the angular output of the IMU is not used for complete biomechanical reconstruction of the lower limbs, but as a geometric feedback variable for switching the FES channels.

3.1.2.3 Manual interface and operational safety

The manual interface consists of the stimulation control and emergency-stop device. The control allows the operator to adjust stimulation current amplitude during the trial, retaining direct control over the amplitude of the applied stimulus. This adjustment is performed by the operator and does not represent automatic current modulation by the system.

The emergency stop is connected to the central control unit and monitored during platform operation. When activated, it interrupts FES-channel activation and permits rapid suspension of stimulation whenever required for experimental or operational reasons. This function operates independently of the intensity adjustment made with the control.

Before each trial, the emergency stop was checked together with the other platform elements. If an interruption was required, the trial was resumed only after the system's operating conditions had been verified. The manual interface therefore combines two complementary functions: stimulation-intensity adjustment and rapid interruption of the stimulus when necessary.

3.1.2.4 FES units and electrical-stimulation output stage

The FES units are responsible for activating the functional electrical-stimulation channels. The architecture uses three ESP32-based units, each associated with two channels, providing six independent outputs in total. This configuration distributes stimulation among the muscle groups involved in pedalling, such as the quadriceps, gluteal and hamstring muscles.

The electrical-stimulation output stage used on this platform was based on the architecture previously developed for FES-Cycling applications by Hernández (2022). In this thesis, the circuit was integrated into the proposed architecture, retaining the logic for generating biphasic current-controlled pulses and adapting its operation to FES-channel activation as a function of the stimulation angular ranges.

During the trials, the FES channels were configured to generate biphasic rectangular pulses comprising positive and negative phases of equal duration. Each phase was set to 500 μs, while the stimulation-generation routine was nominally updated every 20 ms, corresponding to a frequency of 50 Hz. An interval of 50 μs was programmed between the positive and negative phases, in addition to the safety time specified in the H-bridge switching routine. Stimulation amplitude was controlled by the reference signal associated with the digital-to-analogue converter and the current-control stage.

The stimulation parameters were defined in the firmware of the FES units, considering the generation of biphasic rectangular pulses, temporal control of the phases and adjustment of current amplitude. In the comparative trials, the maximum stimulation amplitude was maintained at 34 mA. Table 10 summarises the main parameters used to generate and activate the stimuli.

Table 10 – Main stimulation parameters used on the FES-Cycling platform.

Parameter	**Value/configuration**	**System function**
Waveform	Biphasic rectangular	Apply current with two opposite polarities through the H-bridge.
Number of channels	6 independent channels	Stimulate the quadriceps, gluteal and hamstring muscles of both limbs separately.
Duration of each phase	500 μs	Define the duration of current application for each polarity.
Programmed interval between phases	50 μs	Separate the positive and negative phases of the stimulus in time.
Nominal stimulation frequency	50 Hz	Define the stimulus repetition rate in the active channel.
Nominal update period	20 ms	Define the update interval of the stimulation routine.
Programmed interval between channels	1000 μs	Separate the successive activation of the different channels.
Amplitude control	DAC and current-control stage	Adjust the stimulation current amplitude applied by the FES channel.
Maximum amplitude in the analysed trials	34 mA	Establish the maximum current limit used in the comparative trials.
Activation criterion	Crank angular position	Activate the channel when the crank is within the corresponding stimulation angular range.

Source: Prepared by the author.

Figure 5 presents the functional architecture of the FES stimulator output stage used in this work. The signals S_1, S_2 and S_3 are generated by the ESP32 of the FES unit. Signals S_1 and S_2 control the H-bridge, defining the polarity of the current applied to the electrodes. Signal S_3 acts as an amplitude reference and is applied to the voltage-to-current converter and the Wilson current mirror.

Figure 5 – Functional architecture of the FES stimulator output stage.

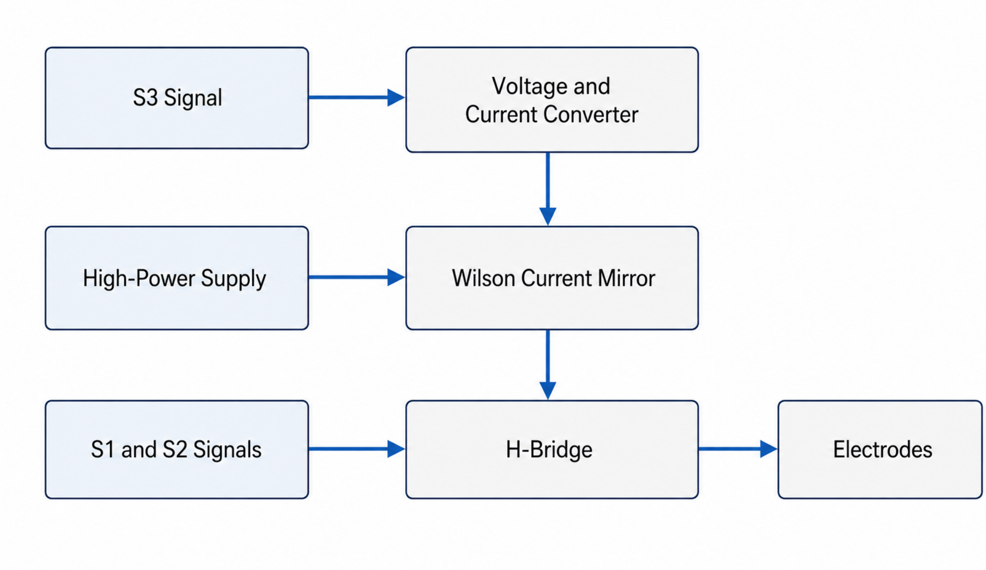

Source: Prepared by the author.

The H-bridge switching logic is defined by two binary signals, $S_1(t)$ and $S_2(t)$, with logical interlocking:

$$S_1(t), S_2(t) \in \{0, 1\}, \qquad S_1(t)S_2(t) = 0. \tag{2}$$

The condition presented in Equation 2 prevents simultaneous activation of the two H-bridge polarities. When $S_1(t) = 1$ and $S_2(t) = 0$, current is applied in one direction; when $S_1(t) = 0$ and $S_2(t) = 1$, the polarity is reversed. During the interpulse interval, both signals remain at a low logic level.

Signal S_3 defines the current reference of the FES channel. This relationship can be represented as follows:

$$I_{\mathrm{ref},i} = f_i(S_3), \tag{3}$$

where $I_{\mathrm{ref},i}$ is the reference current of channel i, and $f_i(\cdot)$ represents the calibration relationship between the command generated by the ESP32 and the current delivered by the output stage.

The stimulation current applied to channel i can be described as follows:

$$I_i(t) = I_{\mathrm{ref},i}\left[S_1(t) - S_2(t)\right]. \tag{4}$$

In Equation 4, $S_1(t)$ represents the positive pulse phase, $S_2(t)$ represents the negative phase and $I_{\mathrm{ref},i}$ defines the current amplitude. Thus, the H-bridge reverses the polarity, while the voltage-to-current converter and the Wilson current mirror regulate stimulus intensity.

The high-voltage supply provides the margin required to compensate for electrode–tissue-interface impedance and maintain regulated current during pulse application. Thus, the electrical-stimulation stage separates amplitude control, associated with S_3, from polarity control, associated with S_1 and S_2, enabling the generation of biphasic rectangular pulses compatible with FES-channel activation within the stimulation ranges defined for the pedalling cycle.

3.1.2.5 System power supply

The platform power supply was organised to separate low-power circuits from the stages associated with electrical stimulation. The control, sensor and communication circuits operate at regulated voltage, whereas the *boost* DC–DC converter supplies the higher voltage required by the FES stage.

This functional separation improves electrical organisation, facilitates fault analysis and contributes to platform operating safety. In addition, the distribution across voltage levels distinguishes the paths associated with processing and communication from those associated with applying the stimulation pulses.

3.1.3 Angular switching logic of the FES channels

Stimulation-range control was structured around crank angular position. Each FES channel is enabled only when the instantaneous angular position lies within the range assigned to the corresponding muscle group.

Let $\theta(t)$ denote the crank angular position at time t, defined over $0^\circ \leq \theta(t) < 360^\circ$. For each muscle group m, a stimulation range is defined by the initial angle $\theta_{i,m}$ and final angle $\theta_{f,m}$. Figure 6 presents the adopted angular convention and the ranges configured for the six FES channels. In the configuration shown, the interval between 0° and 9° is not assigned to any channel, so stimulation remains disabled in this region.

The activation function of the channel associated with muscle group m is

$$u_m(\theta) = \begin{cases} 1, & \text{if } \theta_{i,m} \leq \theta \leq \theta_{f,m}, \\ 0, & \text{otherwise.} \end{cases} \tag{5}$$

In Equation 5, $u_m(\theta) = 1$ indicates an enabled channel, whereas $u_m(\theta) = 0$ indicates a disabled channel. The central unit therefore continuously checks crank position and

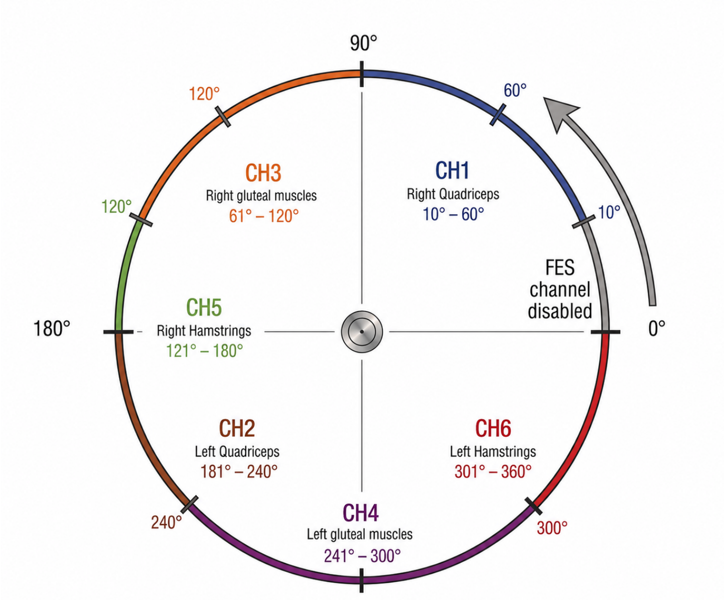

Figure 6 – Crank angular convention and stimulation angular ranges used to activate the FES channels.

Source: Prepared by the author.

enables only the channels whose ranges correspond to the current phase of the cycle.

For ranges crossing the transition between 360° and 0°, the activation condition is

$$u_m(\theta) = \begin{cases} 1, & \text{if } \theta \geq \theta_{i,m} \text{ or } \theta \leq \theta_{f,m}, \\ 0, & \text{otherwise.} \end{cases} \tag{6}$$

This representation accommodates all angular ranges in the pedalling cycle, including those crossing the angular origin. The current applied to channel m can be written as

$$I_m(t) = u_m\big(\theta(t)\big) I_{\text{ref},m}(t), \tag{7}$$

where $I_{\text{ref},m}(t)$ is the reference current defined for the corresponding FES channel. Angular position therefore determines when the channel is activated, while stimulation intensity is adjusted separately through the current reference.

At this stage of development, $\theta_{i,m}$ and $\theta_{f,m}$ are treated as experimental parameters. Current amplitude can be adjusted manually through the stimulation control, retaining direct control of intensity during the trial. The architecture therefore separates two functions: temporal selection of stimulation, determined by the angular ranges, and amplitude adjustment, determined by the manual interface.

This formulation provides the basis for personalising the stimulation ranges. Because movement data, angular limits and pedalling response can be recorded during the trials, different muscle-activation configurations can be evaluated and the ranges can subsequently be adjusted individually using data-analysis and artificial-intelligence methods.

3.1.4 Experimental integration and operational safety

Experimental integration followed a modular approach in which each subsystem was checked independently before unified platform operation. This strategy enabled progressive assessment of IMU-based kinematic acquisition, wireless communication with the central unit, manual-interface response, FES-unit switching and electrical-power distribution.

Operational safety was structured around three complementary measures:

i. **Emergency stop:** responsible for rapidly interrupting system operation and disabling electrical stimulation whenever required for experimental or operational reasons.

ii. **Manual intensity adjustment:** performed through the stimulation control, allowing the operator to adjust current amplitude during the trial.

iii. **Angular-switching logic:** implemented in the firmware to restrict FES-channel activation to the fixed ranges configured for each muscle group.

Functional separation between the logic circuits and the electrical-stimulation stage also supports organisation and safety. The control, sensing and communication modules operate at regulated low voltage, whereas the higher voltage supplied by the *boost* DC–DC converter is restricted to the FES stage and electrode connections. This topology reduces assembly ambiguity, facilitates fault diagnosis and helps mitigate interference between the control and stimulation blocks.

Before integrated trials, a pre-test procedure was used to verify IMU operation, communication with the central unit, emergency-stop response, stimulation-control adjustment, FES-channel activation and continuity of the electrode connections. This verification reduces experimental uncertainty and improves the reproducibility of the test conditions.

The resulting infrastructure provides a functional and modular electronic platform for kinematic acquisition, angular-switching logic and multichannel FES activation. It supplies the technical basis for the experimental protocols, data processing and computational methods supporting stimulation-range personalisation presented in the following chapters.

3.2 EXPERIMENTAL METHODOLOGY AND DATA PROCESSING

3.2.1 Research ethics

Experimental procedures involving human participants were conducted within a project previously submitted for ethical review through Plataforma Brasil. The study involving functional electrical stimulation, photobiomodulation and assisted cycling was approved by the Research Ethics Committee of the Federal University of Mato Grosso do Sul, under Substantiated Opinion no. 6.116.684, linked to CAAE no. 69620023.4.0000.0021.

This ethical approval is relevant because the research involves functional electrical stimulation in an experimental assisted-cycling context. Procedures relating to volunteer participation, data collection and trial execution were therefore conducted within the methodological and ethical limits established by the approved opinion.

In this thesis, the analysis was conducted from a technical and experimental perspective, focusing on electronic-platform development, signal acquisition, data processing and kinematic assessment of the FES-Cycling system. The ethical approval consequently defines the context in which trials involving human participants were conducted without shifting the principal focus towards a clinical or physiological assessment of therapeutic effects.

The document confirming ethical approval is presented in Annex 5.5 as a formal record of the institutional authorisation for the experimental procedures used in this research.

The trials considered in this thesis involved a single participant under the protocol approved by the Research Ethics Committee. Because the study had a technical and experimental focus, the analysis concentrated on platform operation, crank-angle acquisition, stimulation-channel activation and pedalling kinematics. Individual participant characteristics were not used as analytical variables. The results should therefore be interpreted within the evaluated experimental conditions and should not be extrapolated to clinical populations or therapeutic efficacy.

3.2.2 Experimental protocol for the FES-Cycling trials

The experimental protocol was defined to standardise trials with the FES-Cycling platform, ensuring verification of the electronic modules, configuration of stimulation ranges and systematic recording of the experimental variables.

The trials were conducted indoors with the *trike* positioned on a training roller, allowing stationary pedalling. The mechanical platform configuration was maintained throughout the tests to preserve comparable conditions among the trials.

Each trial was treated as an independent experimental unit associated with a specific stimulation, acquisition and storage configuration. This organisation permits comparison of trial conditions, assessment of pedalling regularity and extraction of quantitative metrics for subsequent analysis.

Before each trial, the platform was inspected, including fixation of the embedded modules, verification of the electrical supply, electrode connections and manual-control response. The central control unit, crank-mounted IMU, FES units and data-acquisition system were then initialised.

Stimulation was delivered through pairs of surface electrodes positioned over the muscle groups selected for the protocol: the quadriceps, gluteal muscles and hamstrings, bilaterally. The electrodes were placed over the corresponding muscle regions to favour activation of the muscle group associated with each FES channel. The adopted electrode arrangement is shown in Figure 7.

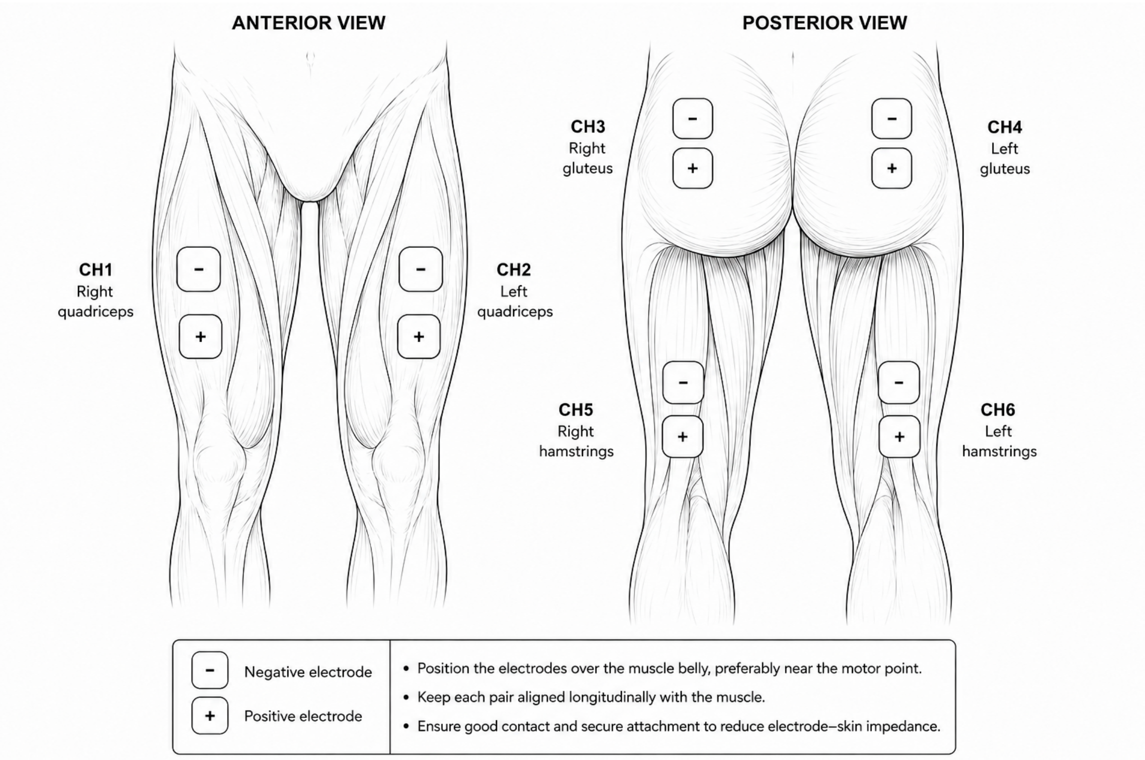

Figure 7 – Surface-electrode placement for bilateral stimulation of the quadriceps, gluteal muscles and hamstrings.

Source: Prepared by the author.

After angular readings and inter-module communication had been confirmed, the predetermined stimulation ranges for each muscle group were configured and kept constant throughout each trial. During execution, the central unit monitored crank position and enabled the FES channels only when the instantaneous angle lay within the range defined for each channel. Stimulation intensity remained adjustable through the manual interface.

The protocol also included criteria for trial interruption. Stimulation could be terminated in the event of communication failure, operational instability, discomfort or any condition incompatible with continuing the trial. In such cases, interruption was performed using the emergency stop or by manually reducing stimulation current amplitude.

The operational sequence of the protocol is presented in Figure 8. The flowchart summarises the steps from platform preparation to storage of the experimental data. The protocol establishes a reproducible routine for conducting the trials, preserving traceability of the experimental conditions and providing the basis for acquisition, organisation, processing and metric extraction.

At this stage of the research, the electromechanical delay between electrical-stimulus application and the effective mechanical pedalling response was treated as a methodological limitation. The angular ranges remained fixed during each trial, without adaptive compensation for cadence, neuromuscular fatigue or individual response. The analysis therefore focused on the observed kinematic response for each experimental configuration.

Figure 8 – Operational flow of the experimental protocol for the FES-Cycling trials.

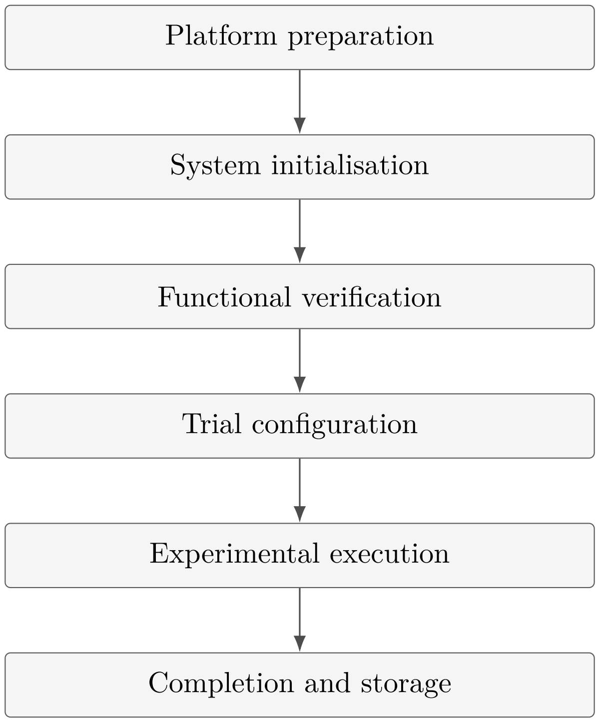

Source: Prepared by the author.

3.2.3 Experimental data acquisition

Experimental data acquisition was structured to record the variables required for analysing the pedalling cycle and synchronising the functional electrical-stimulation channels. The system integrated the crank-mounted IMU, central control unit and FES units, allowing crank angular position to be related to the stimulation ranges defined for each trial.

Inertial data were acquired at 100 Hz, corresponding to a 10 ms sampling period. The FES-logic update routine operated at 50 Hz, with a 20 ms interval. This separation allowed crank movement to be recorded with higher temporal resolution while FES-channel activation remained linked to the angular-activation logic.

During the trials, acquisition time, crank angular position and stimulation parameters were recorded. Angular position was used to identify complete cycles, estimate cadence and enable the FES channels within the corresponding ranges. Acquisition time provided the temporal basis for organising the records and subsequently processing the signals. Table 11 summarises the principal parameters adopted for experimental acquisition.

Table 11 – Main parameters of experimental data acquisition.

Parameter	Specification	Purpose
Inertial sampling	100 Hz (10 ms)	Record crank movement.
FES update rate	50 Hz (20 ms)	Update the FES-channel activation logic.
Recorded variables	Time, angle and FES parameters	Organise the trials and support signal processing.
Angular reference	Crank position	Identify cycles, estimate cadence and enable stimulation ranges.

Source: Prepared by the author.

The acquisition process preserved temporal correspondence among crank movement, angular-range configuration and FES-channel activation. This structure provides the basis for organising the experimental files and processing the signals described in the following sections.

3.2.4 Organisation of the experimental files

The data from each trial were organised into three complementary files separating the temporal pedalling records, stimulation angular parameters and stimulation percentages assigned to the muscle groups. This organisation facilitates test traceability, automatic data reading and comparison between experimental configurations.

Each trial was identified by a common prefix and a letter indicating the type of information stored. Thus, File A, File B and File C were considered for each trial. File A contains the temporal pedalling data; File B stores the stimulation angular ranges; and File C records the percentages assigned to the muscle groups. Table 12 summarises the structure of the experimental files used in the trials.

Table 12 – Structure of the experimental files used in the trials.

File	Main content	Purpose
$File_{\mathrm{A}}$	Time and crank angle	Record the temporal evolution of pedalling.
$File_{\mathrm{B}}$	FES angular ranges	Store the stimulation-range limits.
$File_{\mathrm{C}}$	Stimulation percentages	Record stimulation distribution among the muscle groups.

Source: Prepared by the author.

File A contains the trial's temporal samples, including acquisition time and crank angle. These variables were used to identify complete cycles, estimate cadence, calculate test duration and assess movement regularity.

File B contains the stimulation angular limits for the FES channels. These parameters define the stimulation ranges associated with the quadriceps, gluteal and hamstring muscles on the right and left sides. Table 13 presents the labels used to identify the angular parameters stored in File B.

Table 13 – Angular parameters stored in $File_{\mathrm{B}}$.

Label	Muscle group	Description
RQ_{I}, RQ_{F}	Right quadriceps	Initial and final activation angles.
RG_{I}, RG_{F}	Right gluteal muscles	Initial and final activation angles.
RH_{I}, RH_{F}	Right hamstrings	Initial and final activation angles.
LQ_{I}, LQ_{F}	Left quadriceps	Initial and final activation angles.
LG_{I}, LG_{F}	Left gluteal muscles	Initial and final activation angles.
LH_{I}, LH_{F}	Left hamstrings	Initial and final activation angles.

Source: Prepared by the author.

File C contains the stimulation percentages assigned to the muscle groups considered in the trial. The labels Q, G and H represent the quadriceps, gluteal muscles and hamstrings, respectively. These values complement the experimental configuration by associating each test with the relative distribution of stimulation among the muscle groups.

Separating each trial into three files distinguished the measured variables, stimulation angular parameters and muscle-distribution percentages. This structure made the dataset more suitable for automatic reading, signal processing and extraction of the metrics described in the following sections.

3.2.5 Signal processing

Signal processing was performed using the experimental files generated for each trial. The aim was to transform raw records of time, angular position and stimulation parameters into quantitative variables for pedalling analysis and comparison of experimental configurations.

Initially, the temporal data from $File_{\mathrm{A}}$ were imported and checked for consistency so that invalid samples could be removed. The time and crank-angle sequences were then extracted and used to identify complete pedalling cycles, calculate trial duration and estimate cadence.

Cycles were identified from the crank's angular transition. Because the angle is represented over 0° to 360°, each angular reset marks the beginning of a new cycle. Negative discontinuities in the angular trajectory were therefore used to segment the signal into successive cycles.

The total trial duration was calculated as the difference between the final and initial acquisition times:

$$T_{\mathrm{trial}} = t_{\mathrm{final}} - t_{\mathrm{initial}}. \tag{8}$$

Mean cadence was estimated from the number of complete cycles identified during the trial:

$$C_{\mathrm{rpm}} = \frac{N_{\mathrm{cycles}}}{T_{\mathrm{trial}}} \times 60, \tag{9}$$

where C_{rpm} is mean cadence in revolutions per minute, N_{cycles} is the number of complete pedalling cycles and T_{trial} is total trial duration in seconds.

To estimate instantaneous angular velocity, the crank angle was converted to radians and represented continuously, avoiding discontinuities at the transition between 360° and 0°. Angular velocity was then obtained by numerical differentiation:

$$\omega(t) = \frac{d\theta(t)}{dt}. \tag{10}$$

Instantaneous cadence was calculated from angular velocity:

$$C(t) = \frac{\omega(t)}{2\pi} \times 60. \tag{11}$$

In addition to cadence, metrics related to temporal regularity and movement repeatability were calculated. Periodicity was estimated by comparing successive pedalling cycles after resampling them to the same number of points. Angular-velocity regularity was assessed from variations in $\omega(t)$ throughout the trial, allowing oscillations and irregularities in crank movement to be identified. Table 14 summarises the main signal-processing steps.

Table 14 – Main signal-processing steps.

Step	Purpose
File reading	Import temporal, angular and trial-parameter data.
Invalid-data removal	Exclude incomplete or non-numeric samples.
Cycle segmentation	Identify complete crank revolutions.
Cadence calculation	Estimate mean and instantaneous pedalling rate.
Regularity analysis	Compare successive cycles and assess periodicity.
Metric preparation	Organise the results for trial classification.

Source: Prepared by the author.

The angular parameters from $File_{\mathrm{B}}$ and stimulation percentages from $File_{\mathrm{C}}$ were associated with the results extracted from $File_{\mathrm{A}}$. Each trial could therefore be represented in a single analytical structure containing pedalling kinematics, stimulation angular ranges and the relative distribution of stimulation among the muscle groups.

At the end of processing, the data were organised into tables containing the number of cycles, trial duration, mean cadence, cadence deviation, angular periodicity and indicators of angular-acceleration variation and low-velocity occupancy. These data formed the basis for extracting the experimental metrics and objectively comparing the trials.

3.2.6 Metrics extracted from the trials

The metrics extracted from the trials were defined to quantify pedalling behaviour, assess movement regularity and compare different stimulation configurations. They were calculated from the signals processed in the preceding section, primarily considering acquisition time, crank angle and stimulation parameters associated with each test.

The variability of cadence was used as an indicator of pedalling stability. The standard deviation of instantaneous cadence was calculated as follows:

$$\sigma_C = \sqrt{\frac{1}{n-1}\sum_{k=1}^{n}\left(C_k - \overline{C}\right)^2}, \tag{12}$$

where σ_C is the cadence standard deviation, C_k is instantaneous cadence at sample k, $\overline{C}$ is mean cadence and n is the number of samples considered.

The cadence coefficient of variation was also calculated:

$$CV_C = \frac{\sigma_C}{\overline{C}} \times 100. \tag{13}$$

The coefficient of variation permits comparison of pedalling stability among trials with different mean cadence values. Lower values indicate lower relative dispersion and, therefore, greater movement regularity.

Angular periodicity was assessed by comparing successive pedalling cycles. Complete cycles were resampled to the same number of points, allowing the repeatability of the angular trajectory to be compared between consecutive revolutions. This metric was used to identify trials with more consistent movement patterns.

Angular-velocity regularity was assessed from variation in $\omega(t)$ throughout the trial. Abrupt oscillations indicate greater movement irregularity, whereas smaller variations suggest more continuous pedalling. Table 15 summarises the principal metrics extracted from the trials.

Table 15 – Metrics extracted from the FES-Cycling trials.

Metric	**Symbol**	**Interpretation**
Trial duration	T_{trial}	Total acquisition time of the trial.
Complete cycles	N_{cycles}	Number of complete crank revolutions.
Mean cadence	$\overline{C}$	Mean pedalling rate in rpm.
Cadence deviation	σ_C	Absolute cadence variation during the trial.
Coefficient of variation	CV_C	Relative cadence variation.
Angular periodicity	P_θ	Repeatability between successive cycles.
Angular-velocity regularity	R_ω	Variation in crank angular velocity throughout the trial.
Angular-acceleration variation	E_α	Kinematic indicator associated with abrupt changes in angular movement.
Low-velocity-zone proportion	R_{dz}	Proportion of trial time spent in a low-velocity zone.
Overall angular performance index	S_θ	Combined normalised score used to rank the trials.
FES configuration	–	Angular ranges and stimulation distribution.

Source: Prepared by the author.

The extracted metrics were associated with the angular ranges in $File_{\mathrm{B}}$ and the stimulation percentages in $File_{\mathrm{C}}$. Each trial could therefore be analysed not only through its pedalling kinematics but also through the applied stimulation configuration.

This organisation enabled objective comparison of the trials, identifying configurations with more cycles, greater cadence stability, better angular periodicity and more favourable angular-acceleration and low-velocity indicators. The results formed the basis for trial classification and analysis of stimulation-range personalisation strategies.

3.2.7 Experimental conditions and analysis criteria

The experimental conditions were defined to ensure that the analysed data represented consistent trials of the FES-Cycling platform. Each test was treated as an independent experimental unit associated with a specific configuration of stimulation angular ranges, FES parameters and pedalling-kinematic records.

Trials with complete temporal and angular records, coherent crank-position variation and identifiable complete cycles were considered valid. Trials with missing angular readings, incomplete data, evident acquisition failures or impossible cycle segmentation were excluded.

Data validation was performed by associating the three experimental files. $File_{\mathrm{A}}$ supplied the temporal and angular records; $File_{\mathrm{B}}$ defined the stimulation angular ranges; and $File_{\mathrm{C}}$ indicated the percentage distribution of stimulation among the muscle groups. This correspondence permitted each trial to be analysed from both crank movement and the applied stimulation configuration. Table 16 summarises the criteria adopted for trial validation and analysis.

Table 16 – Criteria adopted for trial validation and analysis.

Criterion	**Application**
Record integrity	Check for complete temporal and angular data.
Angular reading	Confirm coherent crank-position variation.
Complete cycles	Identify complete revolutions for metric calculation.
File association	Relate kinematic records, angular ranges and stimulation percentages.
Pedalling regularity	Assess cadence stability and cycle repeatability.
Trial comparison	Analyse the relationship between different stimulation configurations and kinematic performance.

Source: Prepared by the author.

Trial analysis was based on kinematic indicators, including trial duration, number of complete cycles, mean cadence, cadence variability, angular periodicity, angular-acceleration variation and low-velocity occupancy. These indicators enabled objective comparison of the trials and identification of configurations with greater pedalling stability.

The calculated metrics describe the platform's kinematic behaviour and its relationship with the stimulation configurations used. They should therefore not be interpreted as direct measures of muscle force, physiological fatigue or absolute biomechanical efficiency.

These criteria organised the data analysis to select consistent trials, reduce interference from incomplete records and establish a quantitative basis for comparing experimental configurations.

3.3 ARTIFICIAL INTELLIGENCE IN THE FES-CYCLING SYSTEM

The application of artificial intelligence to the FES-Cycling system developed in this thesis aims to support the personalisation of the angular ranges of functional electrical stimulation. This strategy is based on the premise that fixed muscle-activation ranges may not adequately represent the variations observed across different trials, operating conditions and motor responses induced by stimulation.

In the proposed system, muscle-group activation is performed as a function of crank angular position. Thus, defining the initial and final stimulation angles is critical to the efficiency of assisted pedalling. Small changes in these ranges may alter the mechanical contribution of the stimulated muscles, affecting cadence, movement regularity and the continuity of the pedalling cycles.

The artificial-intelligence approach was incorporated as a tool to support experimental analysis. The model uses kinematic indicators extracted from the trials, such as the number of valid cycles, mean cadence, cadence variability, angular periodicity, angular-acceleration variation and low-velocity occupancy, to estimate angular configurations associated with more favourable kinematic performance. Thus, the neural network does not act directly as a clinical or biomechanical controller, but as a computational resource for pattern identification and support for the personalisation of stimulation angular ranges.

The adopted methodology integrates the processed data from Section 3.2 into a supervised-modelling stage, in which the experimental variables are related to the stimulation angular ranges of the quadriceps, gluteal and hamstring muscles.

Therefore, the use of artificial intelligence in this work does not replace the experimental, biomechanical or physiological validation of the stimulation ranges. Its function is to provide an initial data-based estimate to guide the selection of configurations that are more consistent with the performance observed during the FES-Cycling trials.

3.3.1 Experimental basis for supervised modelling

The database used for supervised modelling was constructed from the experimental trials processed in Section 3.2. At this stage, each trial was treated as an independent sample comprising descriptors of pedalling performance and the corresponding stimulation configurations applied.

The kinematic indicators extracted from the processed signals were organised as model input variables. These indicators included the number of complete cycles, trial duration, mean cadence, cadence variability, angular periodicity, angular-acceleration variation and low-velocity occupancy. These variables summarise pedalling behaviour and enable objective comparison of different experimental conditions.

The output variables were defined from the stimulation angular ranges and the muscle-activation percentages associated with each trial. Accordingly, the model was structured to relate the performance observed during pedalling to the corresponding stimulation configurations for the quadriceps, gluteal and hamstring muscles.

The final database was organised according to a supervised-regression structure, in which the experimental descriptors form the input vector and the stimulation parameters form the output vector. This formulation enabled the neural network to be used as a tool to support the estimation of angular ranges more compatible with the performance observed in the trials.

Only trials with valid records, identifiable complete cycles and consistent correspondence between kinematic data, angular ranges and stimulation percentages were retained in the database. This selection reduced the influence of incomplete or inconsistent records on model training.

3.3.2 Formulation of the regression problem and inverse mapping

The personalisation of the stimulation ranges was formalised as a multivariate supervised-regression problem. In this formulation, each experimental trial i is treated as an independent sample, in which the model seeks to relate the kinematic descriptors of pedalling to the stimulation parameters applied in the FES-Cycling system. The database can be written as

$$\mathcal{D} = \{(\mathbf{x}_i, \mathbf{y}_i)\}_{i=1}^{N}, \qquad \mathbf{x}_i \in \mathbb{R}^9, \quad \mathbf{y}_i \in \mathbb{R}^{15}, \tag{14}$$

where N represents the number of valid trials used in the modelling process.

The input-feature vector comprises the metrics extracted from the crank angular processing. These variables describe cadence, temporal stability, angular periodicity, angular-acceleration variation and low-velocity occupancy during each trial. Thus, for trial i, it is defined as

$$\mathbf{x}_i = \begin{bmatrix} C_{\mathrm{rpm},i} \\ \overline{C}_{\mathrm{inst},i} \\ \sigma_{C,i} \\ P_{\theta,i} \\ E_{\alpha,i} \\ R_{\mathrm{dz},i} \\ N_{\mathrm{cycles},i} \\ T_{\mathrm{trial},i} \\ S_{\theta,i} \end{bmatrix}. \tag{15}$$

In this representation, C_{rpm} is the cadence estimated by cycle counting; $\overline{C}_{\text{inst}}$ and σ_C represent, respectively, the mean and standard deviation of instantaneous cadence; P_θ quantifies angular periodicity between successive cycles; E_α is a kinematic indicator associated with variation in crank angular acceleration; R_{dz} is the proportion of time spent in regions of low angular velocity; N_{cycles} is the number of complete cycles; T_{trial} is the total trial duration; and S_θ is the kinematic score.

The descriptors E_α, R_{dz} and S_θ were included to complement the basic cadence, duration and periodicity metrics. The term E_α penalises abrupt oscillations in angular movement, whereas R_{dz} indicates portions with less effective crank progression. In turn, S_θ summarises trial kinematic performance from the normalised metrics. These descriptors should be interpreted as operational indicators derived from crank kinematics, rather than as direct measures of mechanical energy, torque, power or muscle fatigue.

The output vector contains the stimulation parameters to be estimated by the model. To keep the notation compact, the initial and final angular limits for each muscle group and side are grouped in pairs. For $m \in \mathcal{M} = \{RQ, RG, RH, LQ, LG, LH\}$, define

$$\boldsymbol{\theta}_{m,i} = \begin{bmatrix} \theta^{\mathrm{I}}_{m,i} & \theta^{\mathrm{F}}_{m,i} \end{bmatrix}^{\mathsf{T}}. \tag{16}$$

With this definition, the output vector can be written as

$$\begin{aligned} \mathbf{y}_i = \Big[& \boldsymbol{\theta}^{\mathsf{T}}_{RQ,i}, \boldsymbol{\theta}^{\mathsf{T}}_{RG,i}, \boldsymbol{\theta}^{\mathsf{T}}_{RH,i}, \boldsymbol{\theta}^{\mathsf{T}}_{LQ,i}, \\ & \boldsymbol{\theta}^{\mathsf{T}}_{LG,i}, \boldsymbol{\theta}^{\mathsf{T}}_{LH,i}, p_{Q,i}, p_{G,i}, p_{H,i} \Big]^{\mathsf{T}} \in \mathbb{R}^{15}. \end{aligned} \tag{17}$$

The superscripts I and F indicate the initial and final activation angles, respectively. The letters Q, G and H represent the quadriceps, gluteal and hamstring muscle groups, whereas the prefixes R and L indicate the right and left sides. The terms p_Q, p_G and p_H correspond to the stimulation percentages assigned to each muscle group.

The objective of the model is to approximate a nonlinear function capable of mapping the kinematic descriptors of pedalling to the stimulation parameters. This inverse mapping is written as

$$\begin{gathered} \hat{\mathbf{y}}_i = f_{\mathbf{W}}(\mathbf{x}_i), \\ f_{\mathbf{W}} : \mathbb{R}^9 \to \mathbb{R}^{15}, \end{gathered} \tag{18}$$

where $\hat{\mathbf{y}}_i$ denotes the vector of estimated parameters and $\mathbf{W}$ denotes the set of weights adjusted during supervised training.

In general, the adjustment of the weights can be expressed by minimising the mean squared error between the observed and estimated parameters. With $d_y = 15$, one has

$$
\begin{aligned}
\mathcal{L}(\mathbf{W}) &= \frac{1}{N d_y} \sum_{i=1}^{N} \left\| \mathbf{y}_i - f_{\mathbf{W}}(\mathbf{x}_i) \right\|_2^2 , \\
\mathbf{W}^{\star} &= \arg\min_{\mathbf{W}} \mathcal{L}(\mathbf{W}) .
\end{aligned}
\tag{19}
$$

The loss function $\mathcal{L}(\mathbf{W})$ measures the mean difference between the reference stimulation parameters and the values estimated by the neural network. For each trial i, the term $\mathbf{y}_i - f_{\mathbf{W}}(\mathbf{x}_i)$ represents the model prediction error. The squared Euclidean norm aggregates the errors of all components of the output vector and penalises larger deviations.

The normalisation by Nd_y accounts for the number of experimental samples and the dimension of the output vector. Thus, the loss function represents the mean error per estimated parameter. Minimising $\mathcal{L}(\mathbf{W})$ defines the set of weights $\mathbf{W}^{\star}$ adjusted during supervised training.

Figure 9 summarises the inverse-mapping formulation used in this work. The vector $\mathbf{x}_i \in \mathbb{R}^9$ contains the kinematic descriptors of pedalling, whereas the vector $\mathbf{y}_i \in \mathbb{R}^{15}$ contains the corresponding stimulation parameters. The model $f_{\mathbf{W}}$ relates these two spaces and is trained by minimising the loss function.

Figure 9 – Schematic representation of the inverse mapping used in the formulation of the supervised-regression problem.

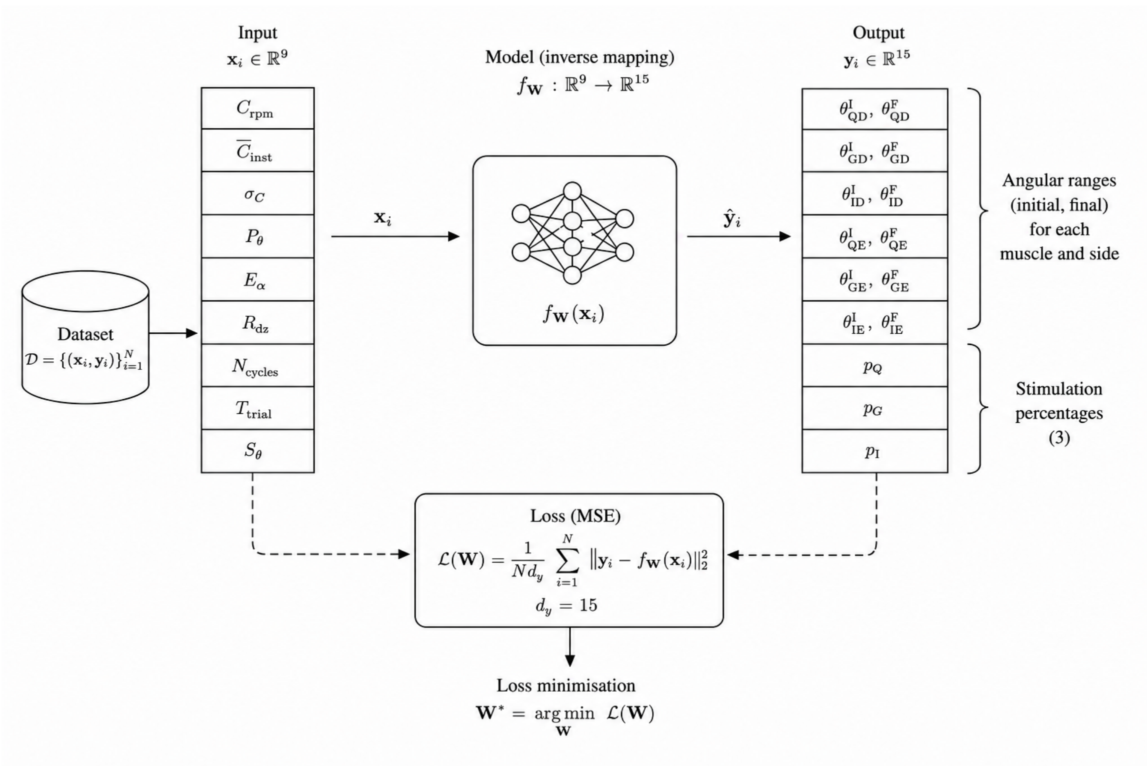

Source: Prepared by the author.

This formulation characterises the problem as multivariate regression, since the model outputs are numerical values associated with the stimulation configurations. The neural network was therefore not used to classify the trials, but to estimate stimulation parameters from the kinematic descriptors extracted from the experimental tests. In this context, the model should be interpreted as an auxiliary analysis and decision-support tool for selecting stimulation ranges, without replacing the experimental assessment of the proposed configurations.

This inverse mapping should be interpreted as an empirical approximation based on the available experimental database, rather than as a unique solution to the problem of personalising the angular ranges. Different stimulation configurations may produce similar kinematic responses; consequently, the neural-network outputs are treated as candidate configurations subject to experimental verification before any practical application.

Although the stimulation percentages form part of the trial parameter vector, the personalisation stage analysed in this thesis focused on the stimulation angular ranges. Thus, the terms p_Q, p_G and p_H were retained in the output structure to preserve the complete representation of the experimental configuration, but the percentages associated with the muscle groups were kept constant in the evaluated inferences. Accordingly, the differences observed in the kinematic metrics were interpreted in relation to changes in the limits of the stimulation angular ranges, without attributing the results to variations in the percentage distribution of stimulation.

3.3.3 MLP neural-network architecture

To solve the supervised-regression problem, a multilayer perceptron artificial neural network, or *Multilayer Perceptron* (MLP), was adopted. This architecture was selected for its ability to approximate nonlinear relationships between input and output variables and its suitability for regression problems involving continuous parameters.

The network was implemented in MATLAB using the *fitnet* function, configured with two hidden layers. The architecture was defined as *fitnet*([15,10]), comprising a first hidden layer with 15 neurons and a second hidden layer with 10 neurons. The output layer was configured for regression, allowing continuous values associated with the stimulation parameters to be estimated.

The network input vector consists of the nine kinematic descriptors defined in Section 3.3.2. These descriptors summarise the angular performance of pedalling in each trial. The output vector comprises the corresponding stimulation parameters, including the angular limits of the stimulation ranges and the stimulation percentages recorded in the experimental structure.

In general, the processing performed by the MLP can be represented as a sequence of linear transformations followed by nonlinear activation functions in the hidden layers. For an input $\mathbf{x}_i$, the network forward propagation can be expressed as follows:

$$\begin{aligned} \mathbf{h}_{1,i} &= \phi_1\left(\mathbf{W}_1\mathbf{x}_i + \mathbf{b}_1\right), \\ \mathbf{h}_{2,i} &= \phi_2\left(\mathbf{W}_2\mathbf{h}_{1,i} + \mathbf{b}_2\right), \\ \hat{\mathbf{y}}_i &= \mathbf{W}_3\mathbf{h}_{2,i} + \mathbf{b}_3. \end{aligned} \tag{20}$$

In this representation, $\mathbf{h}_{1,i}$ and $\mathbf{h}_{2,i}$ correspond to the activations of the first and second hidden layers, respectively. The matrices $\mathbf{W}_1$, $\mathbf{W}_2$ and $\mathbf{W}_3$ represent the network synaptic weights, whereas $\mathbf{b}_1$, $\mathbf{b}_2$ and $\mathbf{b}_3$ represent the bias vectors. The functions $\phi_1(\cdot)$ and $\phi_2(\cdot)$ introduce nonlinearity into the model, enabling the approximation of complex relationships between the kinematic descriptors and stimulation parameters.

The output of the final layer was kept linear because the problem was formulated as regression. This choice preserves the continuous scale of the estimated variables, expressed in degrees and percentages, without imposing discrete classes on the result. Thus, the neural network directly estimates the stimulation parameters from the kinematic characteristics of each trial.

The adopted architecture was used as an exploratory approach to investigate the relationship between the kinematic descriptors and the stimulation parameters. Given the limited size of the experimental database, the estimates provided by the MLP were used to support the definition of candidate configurations, which were subsequently subjected to experimental assessment.

3.3.4 Neural-network training, validation and testing

The neural network was trained in a supervised manner using the input-output pairs defined from the experimental database. Each sample associated the kinematic descriptors of pedalling with the corresponding stimulation parameters recorded in the trial.

The database was divided into three subsets: training, validation and testing. The training subset was used to adjust the network weights and biases, whereas the validation set enabled the evolution of the error to be monitored during the learning process. The test set was reserved for evaluating model behaviour on samples that did not directly participate in adjusting the network parameters.

The adopted partition comprised 70% of the samples for training, 15% for validation and 15% for testing, following the structure used in the training procedure of the *fitnet* function.

During training, the internal network parameters were adjusted to minimise the mean squared error between the reference and estimated outputs. The validation error was monitored throughout this process, helping to stop training when no further improvement in model performance was observed and reducing the risk of overfitting.

Because the experimental database used in this work is limited in size, the neural-network results were interpreted conservatively. In this context, the model outputs were used as auxiliary estimates to support the selection of new stimulation angular ranges, without assuming generalisation to different individuals or experimental conditions. The configurations suggested by the network were subsequently evaluated on the FES-Cycling platform itself. Expanding the experimental database with a larger number of trials and different test conditions may enable a more comprehensive assessment of the model's robustness and generalisation capability.

3.3.5 Trial ranking and selection of reference configurations

After signal processing and organisation of the experimental database, the trials were ranked to identify the stimulation configurations associated with the best kinematic pedalling performance. This ranking was used as an auxiliary stage to guide the selection of reference configurations and support the inferences performed by the neural network.

The ranking criterion was based exclusively on metrics extracted from crank angular behaviour. Variables related to cadence, rhythm stability, periodicity between cycles, angular-acceleration variation and pedalling continuity were considered. Thus, the assessment prioritised the observed kinematic performance without using direct physiological measures of muscle force or fatigue.

To synthesise these metrics into a single indicator, a combined score denoted by S_θ was used. This index brought normalised metrics together on a common scale, assigning higher scores to trials with higher cadence and periodicity, lower variability, a lower indicator associated with variation in angular acceleration and less time spent in a low-velocity zone.

In general, the score can be represented as follows:

$$\begin{aligned} S_\theta = {} & w_{\mathrm{rpm}}\widetilde{C}_{\mathrm{rpm}} + w_{\mathrm{stab}}\left(1-\widetilde{\sigma}_C\right) + w_{\mathrm{per}}\widetilde{P}_\theta \\ & + w_\alpha\left(1-\widetilde{E}_\alpha\right) + w_{\mathrm{dz}}\left(1-\widetilde{R}_{\mathrm{dz}}\right), \end{aligned} \tag{21}$$

where $\widetilde{C}_{\mathrm{rpm}}$, $\widetilde{\sigma}_C$, $\widetilde{P}_\theta$, $\widetilde{E}_\alpha$ and $\widetilde{R}_{\mathrm{dz}}$ represent, respectively, the normalised versions of cadence, cadence deviation, angular periodicity, the indicator associated with variation in angular acceleration and the proportion of time spent in a low-velocity zone. The coefficients w_{rpm}, w_{stab}, w_{per}, w_α and w_{dz} define the weights assigned to each metric.

The score weights were defined heuristically, based on the technical and experimental priority assigned to pedalling continuity, cadence, temporal stability and angular repeatability. This choice was adopted to synthesise different kinematic descriptors into a single trial-ranking criterion. Therefore, the score S_θ should be interpreted as an internal indicator for comparing experimental configurations, rather than as an absolute clinical, physiological or biomechanical metric.

The final ordering of the trials considered, in sequence, the number of complete cycles, mean cadence and the kinematic score. Thus, trials with greater pedalling continuity were prioritised; when the number of cycles was equivalent, mean cadence was used as a supplementary criterion. The kinematic score was employed as an additional indicator for ordering configurations with similar kinematic performance.

$$\text{Ranking} = \text{sort}\left(N_{\text{cycles}}, C_{\text{rpm}}, S_\theta\right)_{\text{desc}}. \tag{22}$$

This procedure enabled objective selection of the trials with the best kinematic performance within the analysed database. The configurations associated with the highest-ranked trials were then used as references for the inference stage and for assessing the stimulation ranges suggested by the model.

3.3.6 Inference and post-processing of the stimulation ranges

After training the neural network, the model was used to estimate candidate stimulation configurations from the kinematic descriptors of the trials. The inference stage consisted of applying the input vector to the trained model, resulting in an output vector containing the parameters associated with the experimental configuration, with the analysis focused on the angular limits of the stimulation ranges.

For a new input sample $\mathbf{x}_{\text{new}}$, the model prediction can be represented as follows:

$$\hat{\mathbf{y}}_{\text{new}} = f_{\mathbf{W}^\star}\left(\mathbf{x}_{\text{new}}\right), \tag{23}$$

where $\mathbf{W}^\star$ denotes the set of weights obtained after training and $\hat{\mathbf{y}}_{\text{new}}$ corresponds to the vector of parameters estimated by the neural network.

The estimated outputs were subjected to post-processing to ensure consistency with the experimental application. This stage included rounding the angular values, checking the physical limits of the pedalling cycle and organising the initial and final angles of each stimulation range. Since FES activation is defined as a function of crank angular position, the estimated values must remain within the interval from 0° to 360°.

The need to preserve consistency between the angle pairs defining each range was also considered. Thus, each muscle group was represented by an initial and a final activation angle, avoiding ambiguous interpretations of the network outputs. When necessary, the estimated values were adjusted to maintain configuration consistency before experimental assessment.

The configurations resulting from inference were not treated as autonomous control commands, but as candidate suggestions for analysis and testing. Thus, the neural network acted as an auxiliary tool to reduce the experimental search space and guide the selection of new stimulation ranges, while retaining the need for practical verification of the proposed configurations.

This approach enables the knowledge acquired from previous trials to be used to propose adjustments to the stimulation ranges without automatically changing the system safety logic. Therefore, the inference stage provides an initial data-based estimate, whereas configuration validation remains dependent on experimental analysis of pedalling performance.

3.3.7 Methodological considerations regarding the use of artificial intelligence

The application of artificial intelligence in this work was delimited to an auxiliary stage for modelling and analysing the experimental data. The neural network was not used as an autonomous controller of the FES-Cycling system, but as a tool to support the estimation of candidate configurations from the kinematic descriptors of pedalling.

The metrics used in the model were extracted from crank angular behaviour. Accordingly, the results estimated by the network should be interpreted as recommendations based on the observed kinematic performance, rather than as direct measures of muscle force, physiological fatigue or absolute biomechanical efficiency.

The personalisation analysed focused primarily on the stimulation angular ranges. Although the stimulation percentages form part of the trial parameter structure, they were kept constant in the evaluated inferences. Thus, the analysis of performance differences was conducted mainly in relation to changes in the stimulation angular ranges.

The configurations suggested by the model require experimental verification before any practical application, since the response to FES may vary according to factors such as electrode placement, muscle condition, fatigue, user posture and the mechanical characteristics of the platform.

Accordingly, the proposed approach should be understood as a method to support the selection and personalisation of stimulation angular ranges. Its contribution lies in organising the experimental data, identifying relationships between kinematic performance and stimulation configurations, and guiding the definition of new test conditions in a more systematic manner.

4 RESULTS AND DISCUSSION

This chapter presents the experimental results obtained with the FES-Cycling platform. The analysis considers crank angular acquisition, activation of the FES channels, pedalling kinematic performance and personalisation of stimulation angular ranges using artificial intelligence.

The results are first presented on the basis of metrics extracted from the trials. The critical discussion, including comparison with the literature, is developed in a subsequent section.

4.1 EXPERIMENTAL RESULTS

The results were organised from trials performed with one volunteer in an indoor environment using the *trike* on a training roller. Stage 1 consisted of a preliminary exploratory trial used to assess the overall pedalling response to manual adjustment of stimulation amplitude and to confirm integrated platform operation. The comparative analysis in this chapter focuses on Stage 2, comprising five initial trials identified as Ti3, Ti4, Ti5, Ti6 and Ti7, followed by trials T8 and T9, obtained using the ranges suggested by the neural network.

In the Stage 2 tests analysed, the maximum amplitude was maintained at 34 mA, with stimulation percentages of 60% for the quadriceps, 70% for the gluteal muscles and 100% for the hamstrings. The comparison among Ti3–Ti7, T8 and T9 was therefore conducted primarily as a function of variations in the stimulation angular ranges.

The metrics analysed were interpreted as indicators of pedalling kinematic performance and of the platform's experimental response. The results were therefore not treated as direct measures of muscle force, physiological fatigue or absolute biomechanical efficiency.

4.1.1 Operational evaluation of the FES-Cycling platform

The operational evaluation of the platform was based on the relationship among crank angular position, the configured stimulation ranges and the pedalling cycles recorded in the Stage 2 tests. Five initial configurations, identified as Ti3, Ti4, Ti5, Ti6 and Ti7, were evaluated in this stage.

Figure 10 presents the crank angular evolution in the five initial tests. The colours overlaid on the angular curves indicate the stimulation ranges associated with each muscle group. This representation allows the occurrence of pedalling cycles to be verified and the

Figure 10 – Crank angular response and stimulation angular ranges in the initial Stage 2 tests. The colours indicate the stimulated muscle groups: RQ, right quadriceps; RG, right gluteal muscles; RH, right hamstrings; LQ, left quadriceps; LG, left gluteal muscles; LH, left hamstrings.

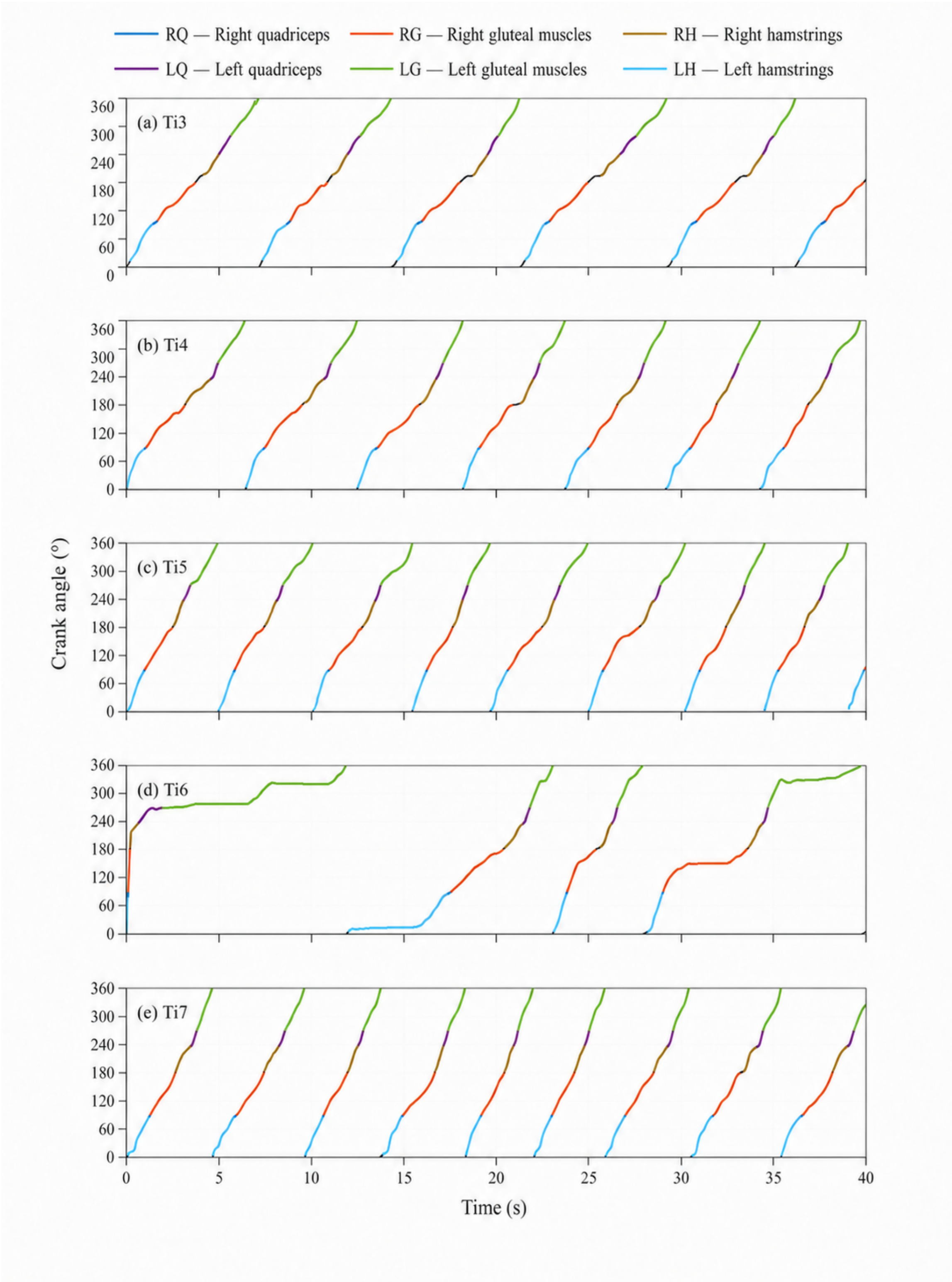

Source: Prepared by the author from the experimental data.

regularity of the evaluated configurations to be compared visually.

Among the initial tests, Ti7, shown in Figure 10(e), exhibited the most regular response, with the greatest number of complete cycles and the highest cadence. In contrast, Ti6, shown in Figure 10(d), exhibited lower movement continuity, with prolonged intervals without effective angular progression.

The quantitative comparison confirms this distinction. Test Ti6 produced 4 complete cycles, a cadence of 5.6 rpm and a score of 0.0967, whereas test Ti7 produced 9 complete cycles, a cadence of 13.4 rpm and a score of 0.8407. These results indicate that the records obtained by the platform were sufficient to distinguish configurations with lower and higher kinematic performance.

4.1.2 Kinematic performance and trial ranking

The kinematic performance of the trials was evaluated using test duration, number of complete cycles, mean cadence and the kinematic score. Table 17 presents the final ranking of the Stage 2 tests.

Table 17 – Ranking of Stage 2 trials based on kinematic indicators.

Rank	Test	Duration (s)	Cycles	Cadence (rpm)	Kinematic score
1	T9	41.85	11	15.8	0.9892
2	T8	43.51	11	15.2	0.9515
3	Ti7	40.29	9	13.4	0.8407
4	Ti5	43.71	9	12.4	0.8109
5	Ti4	39.70	7	10.6	0.7379
6	Ti3	43.24	6	8.3	0.6931
7	Ti6	42.88	4	5.6	0.0967

Source: Prepared by the author from the experimental data.

Test T9 exhibited the best kinematic performance among the evaluated trials, with 11 complete cycles, a cadence of 15.8 rpm and a kinematic score of 0.9892. Test T8 ranked second, also with 11 complete cycles, a cadence of 15.2 rpm and a score of 0.9515. Among the initial tests, Ti7 produced the best result, with 9 complete cycles, a cadence of 13.4 rpm and a score of 0.8407.

Figure 11 shows the Ti7–T8–T9 progression. Although T8 and T9 had the same number of complete cycles, T9 completed the 11 cycles in less time, resulting in a higher mean cadence.

Compared with Ti7, test T9 showed an approximately 18% increase in mean cadence. Compared with Ti6, the test with the lowest kinematic performance, the increase in mean cadence was approximately 180%. Since the maximum stimulation amplitude was

Figure 11 – Evolution of cadence and the kinematic score across the reference and post-inference trials.

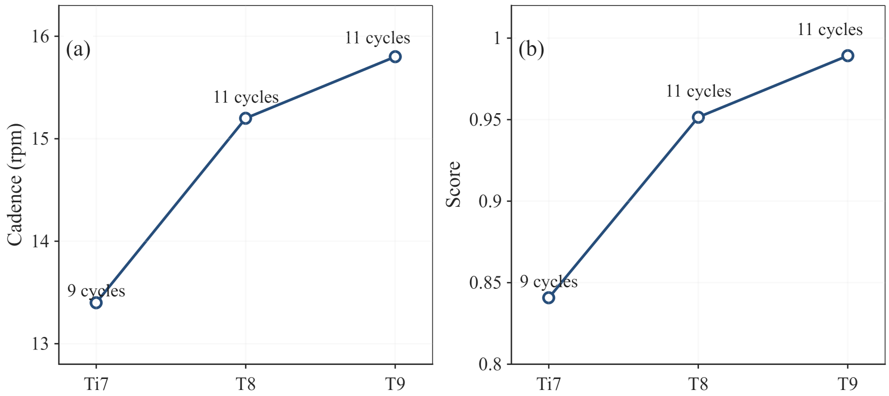

Source: Prepared by the author from the experimental data.

maintained at 34 mA, this difference was interpreted, under the evaluated conditions, as being associated with adjustment of the stimulation angular ranges.

4.1.3 Results of stimulation-range personalisation using artificial intelligence

Artificial-intelligence-based personalisation was initiated from the best initial test, Ti7. After the first inference, the neural network suggested new angular ranges, which were evaluated in test T8. The T8 data were then incorporated into the experimental dataset, generating a second inference and test T9.

Table 18 presents the reference configuration and the angular ranges obtained after the two inferences.

Table 18 – Stimulation angular ranges associated with the reference test and neural-network inferences.

Configuration	**RQ** (°)	**RG** (°)	**RH** (°)	**LQ** (°)	**LG** (°)	**LH** (°)
Ti7	55–170	90–180	185–265	235–350	270–360	5–85
T8	54–184	99–180	189–268	247–359	275–359	5–85
T9	54–184	99–180	189–268	234–360/0–4	279–360	9–88

Source: Prepared by the author from the experimental data and neural-network inference results.

Table 18 reports the stimulation ranges associated with the reference trial and with the configurations evaluated after the two neural-network inferences. The temporal plots in Figures 10, 13 and 14 display the stimulation ranges stored in the corresponding experimental trial files. The table therefore describes the reference and post-processed configurations, whereas the plots document the ranges actually stored for the executed trials; raw neural-network outputs are not reported as if they were directly implemented values.

Figure 12 – Circular representation of the stimulation angular ranges associated with the reference test and the configurations suggested by the neural network. The colours indicate the stimulated muscle groups: RQ, right quadriceps; RG, right gluteal muscles; RH, right hamstrings; LQ, left quadriceps; LG, left gluteal muscles; LH, left hamstrings.

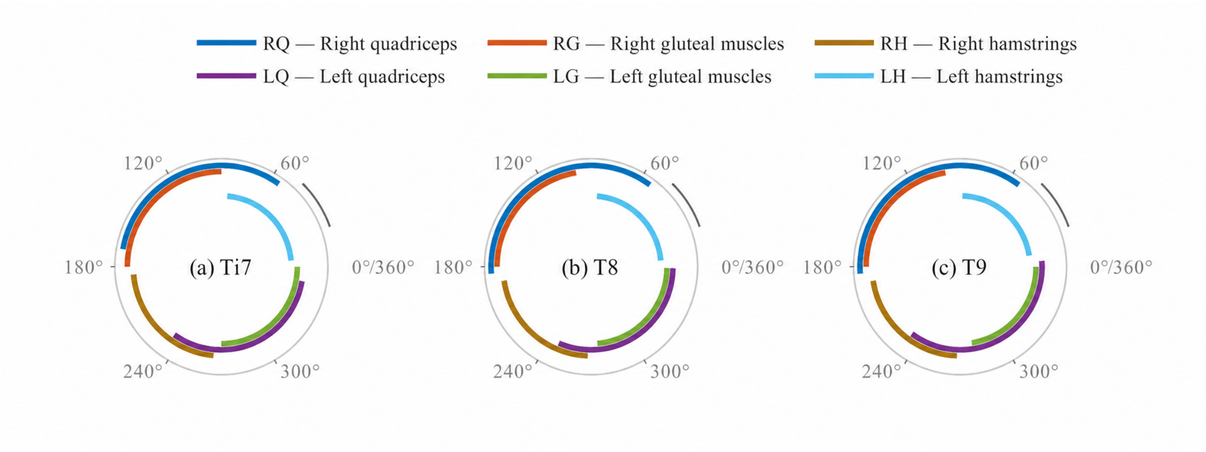

Source: Prepared by the author from the neural-network inference results.

Figure 12 shows the redistribution of angular ranges among Ti7, T8 and T9. The first inference expanded the right-quadriceps range from 55°–170° to 54°–184° and readjusted the remaining ranges. The second inference preserved the RQ, RG and RH ranges and mainly modified the LQ, LG and LH ranges.

Figure 13 – Crank angular response and stimulation angular ranges in test T8 after the first neural-network inference.

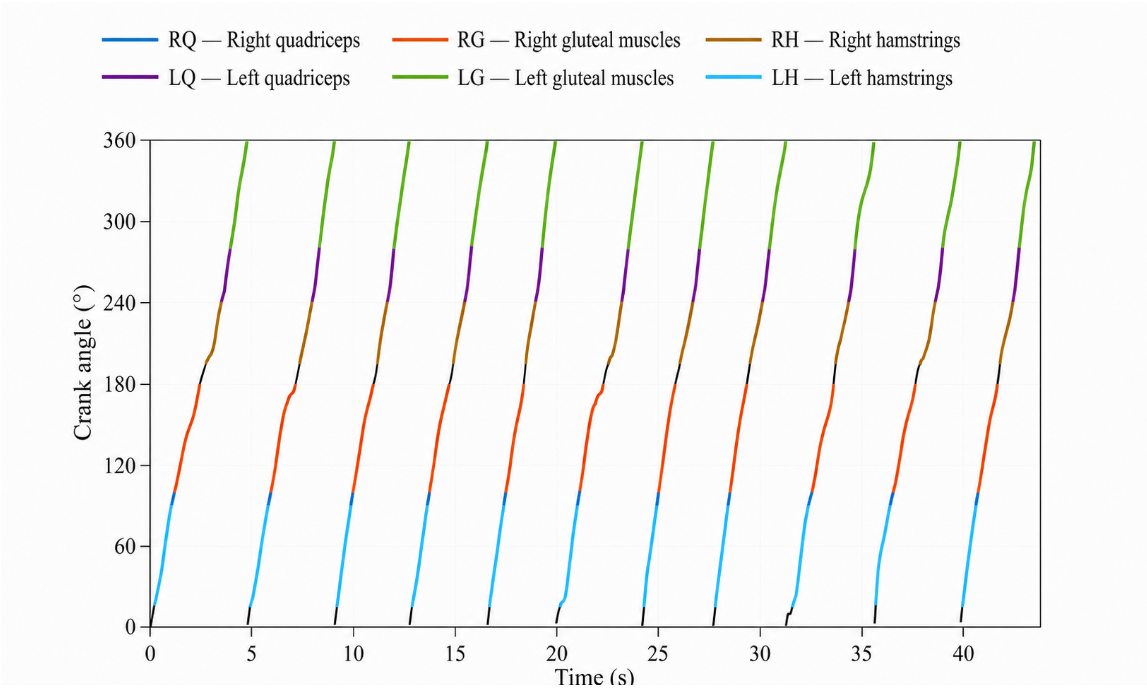

Source: Prepared by the author from the experimental data.

Figure 14 – Crank angular response and stimulation angular ranges in test T9 after the second neural-network inference.

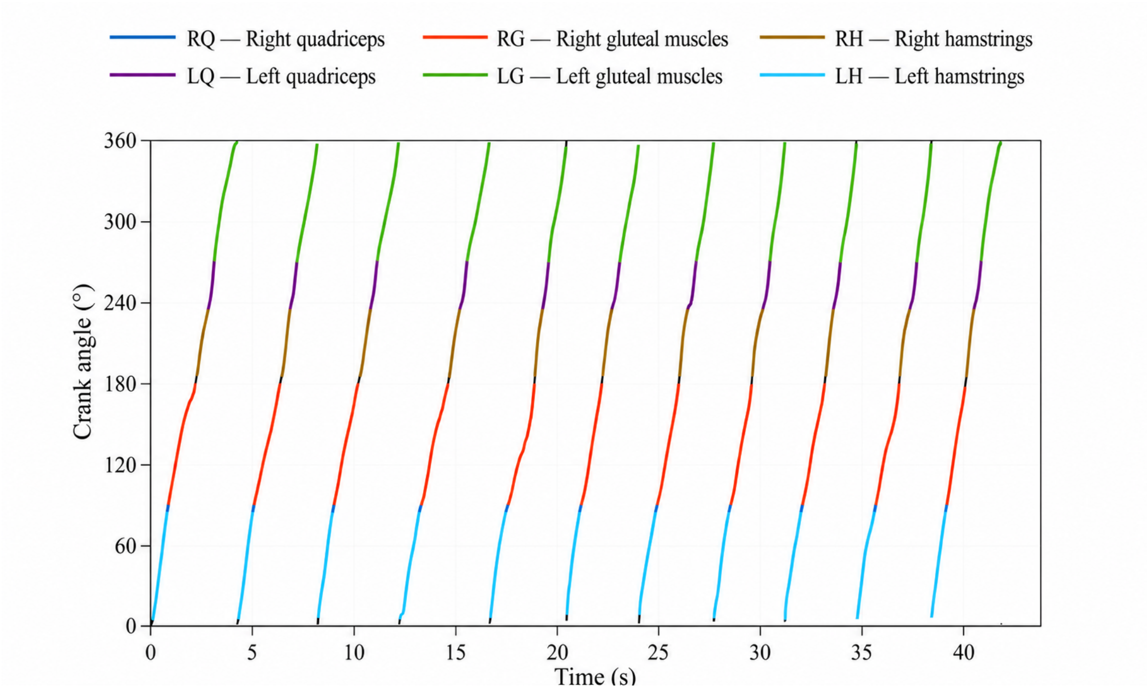

Source: Prepared by the author from the experimental data.

Figures 13 and 14 present the angular responses obtained in tests T8 and T9 after the neural-network inferences. The Ti7–T8–T9 progression showed increases in cadence and the kinematic score without an increase in maximum stimulation amplitude. Under the experimental conditions evaluated, the improvement in kinematic performance was therefore associated with the adjusted angular ranges; because the study used a sequential single-participant design, this result does not establish that the neural network itself caused the improvement.

4.2 DISCUSSION

4.2.1 Interpretation of the trials' kinematic response

The results indicate that the platform was capable of discriminating kinematic differences among different stimulation angular-range configurations. Among the initial Stage 2 tests, Ti6 exhibited the lowest pedalling continuity, with 4 complete cycles, a cadence of 5.6 rpm and a score of 0.0967. In contrast, Ti7 exhibited the best initial performance, with 9 complete cycles, a cadence of 13.4 rpm and a score of 0.8407.

This difference indicates that the pedalling response depended not only on the application of electrical stimulation but also on synchronisation between instantaneous crank angular position and the stimulation angular ranges of the muscle groups. Since the initial tests were conducted with the same maximum current amplitude of 34 mA and the same stimulation percentages for each muscle group, the variation in kinematic performance was mainly associated with the arrangement of the angular ranges.

Less favourable configurations, such as that of Ti6, exhibited lower movement continuity and fewer complete cycles. This behaviour suggests that certain combinations of angular ranges may hinder the crank's kinematic progression throughout the cycle, particularly when activation occurs in regions that are less favourable to the observed angular advance.

After the offline inference and experimental adjustment of the stimulation ranges, tests T8 and T9 performed better than the best initial test, Ti7. Both recorded 11 complete cycles; however, T9 completed these cycles in less time, resulting in a higher mean cadence of 15.8 rpm and a higher score of 0.9892. This progression shows that the configurations evaluated after inference were associated with greater pedalling continuity and regularity under the experimental conditions. It does not, by itself, isolate the effect of the neural network from order effects, participant learning, fatigue, manual adjustments or other uncontrolled factors.

The results therefore support the hypothesis that crank angular feedback provides an appropriate kinematic basis for comparing stimulation configurations and guiding personalisation of angular ranges. In accordance with the design constraints, this interpretation remains restricted to the platform's kinematic and operational performance and does not directly infer muscle force, net torque, physiological fatigue or the user's absolute biomechanical efficiency.

4.2.2 Association between stimulation angular ranges and kinematic performance

The comparison among Ti7, T8 and T9 indicates that kinematic performance was sensitive to repositioning of the stimulation angular ranges. Since maximum current amplitude was maintained at 34 mA and stimulation percentages remained constant in the tests analysed, the observed improvement was associated with adjustment of the stimulation angular ranges rather than with an increase in electrical intensity. Given the sequential single-participant design, this interpretation should not be regarded as definitive causal evidence.

In the first inference, the right-quadriceps range was expanded from 55°–170° in Ti7 to 54°–184° in T8. The limits of the gluteal and hamstring stimulation angular ranges were also adjusted. This new configuration increased the number of complete cycles from 9 in Ti7 to 11 in T8 and increased cadence from 13.4 rpm to 15.2 rpm.

In the second inference, the RQ, RG and RH ranges were preserved relative to T8, whereas the LQ, LG and LH ranges were readjusted. T9 exhibited a more balanced angular distribution between the right and left sides: RQ and LQ occupied 130° of the cycle, RG and LG occupied 81°, and RH and LH occupied 79°. This geometric correspondence between sides does not imply biomechanical symmetry, equal torque or equivalent force between the limbs; it indicates greater regularity in the distribution of the stimulation angular ranges.

Figure 12 complements Table 18 by showing the redistribution of the ranges throughout the complete crank cycle. In T9, the LQ range crosses the angular origin and is represented as 234°–360°/0°–4°; it should be interpreted as continuous activation from 234° to 360° and from 0° to 4°. This treatment preserves cycle continuity and avoids a discontinuous interpretation of activation.

The progressive performance improvement from Ti7 to T8 and T9 suggests that the angular activation position of the muscle groups played an important role in pedalling continuity. The results therefore reinforce that, in FES-Cycling, the choice of angular ranges should be treated as a critical design parameter rather than merely as an auxiliary experimental-protocol setting.

4.2.3 Contribution of artificial intelligence to personalisation

In this thesis, artificial intelligence acted as a decision-support layer rather than as an autonomous adaptive real-time control algorithm for the FES-Cycling platform.

The multilayer perceptron (MLP) model was implemented to relate the trials' kinematic descriptors to their respective stimulation configurations, allowing new angular ranges to be suggested from the processed experimental data.

The Ti7–T8–T9 sequence illustrates this data-driven refinement process. Test Ti7 was selected as the best initial configuration and served as the reference for the first network inference. The suggested configuration was evaluated experimentally in test T8, which showed increases in the number of complete cycles, mean cadence and kinematic score relative to Ti7. The T8 data were then incorporated into the experimental dataset, enabling a second inference that was subsequently evaluated in test T9.

Test T9 exhibited the best kinematic performance within the evaluated set, with 11 complete cycles, a mean cadence of 15.8 rpm and a score of 0.9892. This result shows that the offline experimental-feedback process led to a more favourable configuration within the evaluated set. Since maximum current amplitude was maintained at 34 mA, the kinematic gain observed relative to Ti7 was associated with the readjustment of the angular ranges evaluated after inference, rather than with an increase in applied electrical intensity. However, the sequential design does not permit the independent causal contribution of the neural network to be established.

The adopted approach preserved the separation between computational inference and experimental validation. The ranges suggested by the MLP were not applied as automatic online-control commands; they were treated as candidate configurations whose feasibility was tested on the physical platform. This strategy reduces the risk of overestimating model output and keeps the final evaluation criterion linked to the observed kinematic response.

The contribution of artificial intelligence in this thesis therefore lies in structuring a reproducible procedure to reduce dependence on purely empirical adjustment of stimulation angular ranges. The model transformed experimental records into testable recommendations, establishing an engineering basis for future optimisation strategies supported by larger datasets, complementary sensors and adaptive methods.

4.3 COMPARISON WITH RECENT STIMULATION-PERSONALISATION METHODOLOGIES

The results presented in this chapter indicate that stimulation angular ranges should not be treated as fixed and universal parameters. The variability observed among the trials, both in terms of kinematic regularity and relative performance, indicates that small changes in activation angles may modify the platform's kinematic and operational response. This behaviour is consistent with recent literature, which has sought to replace empirical adjustment with procedures based on data, torque, biomechanical models or computational learning (Schmoll *et al.*, 2022; Coelho-Magalhães, Coste and Resende-Martins, 2022; Wannawas and Faisal, 2023).

In the work of Schmoll *et al.* (2022), stimulation ranges are defined from the direct mechanical contribution of each muscle, estimated using positive net torque. As discussed in Section 2.7, this approach provides a strong biomechanical interpretation because it associates muscle activation with effective torque generation at the crank. In contrast, the methodology in this thesis does not use direct torque measurement; its contribution lies in structuring a kinematic and operational experimental basis capable of ranking trials and supplying a supervised model for recommending stimulation angular ranges. Thus, whereas OIDA prioritises local mechanical identification of each muscle, this thesis prioritises global selection of the stimulation pattern based on observed pedalling-cycle performance.

The approach of Coelho-Magalhães, Coste and Resende-Martins (2022) addresses a different level of the problem. The authors retain a baseline activation pattern and use reinforcement learning to modify amplitude and pulse width during the session, while a PI controller tracks the reference cadence. This strategy is intended for online adaptation of electrical parameters in response to temporal variation in the muscular response. The results of this thesis differ from that approach because learning does not occur during the session and does not alter stimulation in real time.

The approach proposed here is offline: data collected during the trials are processed, classified and used to train an MLP capable of suggesting stimulation angular ranges. The contribution therefore does not lie in instantaneous adaptive control but in transforming experimental records into a reproducible procedure for initial personalisation.

The method of Wannawas and Faisal (2023) is close to this thesis in its use of real data to refine stimulation patterns. However, that strategy begins with a personalised musculoskeletal model in OpenSim and applies reinforcement learning to generate and adjust the activation pattern. This thesis did not adopt an external biomechanical model. Personalisation was based directly on data generated by the platform, preserving consistency among the hardware, experimental protocol and neural-network input variables. This choice reduces dependence on detailed anatomical modelling, although it also limits the absolute biomechanical interpretation of the estimated ranges.

Table 19 summarises the relationship between recent methodologies and the approach developed in this thesis. The comparison is not intended to establish quantitative superiority among methods because the studies differ in participants, sensors, platforms, control variables and experimental protocols. Its purpose is to position the contribution of this study relative to strategies currently used to reduce empirical adjustment of stimulation in FES-Cycling.

Table 19 – Comparison of recent personalisation methodologies with the approach adopted in this thesis.

Source	**Methodological focus**	**Reported result**	**Relationship to this thesis**
Schmoll *et al.* (2022)	Automatic range detection using positive net torque.	Bilateral identification of quadriceps and hamstring ranges, with stable cycling for 5 minutes without further adaptation.	Confirms the importance of defining muscle-specific ranges; this thesis proposes an alternative based on kinematic and operational data without direct torque measurement.
Coelho-Magalhães, Coste and Resende-Martins (2022)	PI cadence control combined with reinforcement learning to adjust amplitude and pulse width.	Under higher loads, sessions with RL enabled covered greater distances than sessions using PI alone.	Reinforces the need to adapt stimulation parameters; this thesis acts before the session by suggesting initial angular ranges from ranked trials.
Wannawas and Faisal (2023)	Reinforcement learning in an OpenSim model followed by fine-tuning with real data.	The pattern refined with 100 s of real data achieved a higher mean speed than the EMG-based and model-only patterns.	Shows that real data can improve stimulation patterns; this thesis follows this direction using experimental data from the platform itself to train an MLP.
This thesis	Experimental ranking and supervised regression to suggest stimulation angular ranges.	Organisation of trials using performance metrics and generation of recommendations through an MLP network.	Contributes an offline, traceable methodology integrated with the developed platform for initial stimulation-range personalisation.

Source: Prepared by the author.

The comparison shows that the proposed methodology occupies an intermediate position between purely biomechanical methods and real-time adaptive strategies. Relative to OIDA, the main limitation of this thesis is the absence of direct torque measurement, which prevents claiming that the suggested ranges necessarily correspond to the intervals of greatest positive net torque. Conversely, the proposed approach reduces instrumentation complexity and exploits kinematic and operational information available from the platform itself, such as angular position, cadence, number of cycles and movement regularity.

Relative to reinforcement-learning-based strategies, the main difference concerns the timing of adaptation. The studies by Coelho-Magalhães, Coste and Resende-Martins (2022) and Wannawas and Faisal (2023) use learning to modify or refine stimulation patterns through interaction with the system or a model. In this thesis, learning is supervised and performed after trial processing. This decision makes the method less adaptive during the session but simpler to validate experimentally because it separates acquisition, ranking, training and recommendation.

The results obtained in this chapter should therefore be interpreted as an initial stage of data-driven personalisation. The developed platform enabled trials to be recorded, consistent metrics to be extracted and a relationship to be established between stimulation patterns and kinematic performance. The MLP does not replace a real-time adaptive-control strategy for torque, cadence, fatigue or current amplitude, nor a torque-based biomechanical analysis. It acts as a decision-support layer capable of suggesting more informed initial configurations than purely empirical adjustment.

This contribution is relevant because it creates a methodological basis for future developments. The same structure could incorporate torque sensors, energy-cost criteria, fatigue estimation or online adaptation of electrical parameters in subsequent studies. The results of this thesis therefore follow the trend observed in recent literature: transforming stimulation personalisation into a measurable, traceable and progressively automatable problem while maintaining compatibility with an experimental platform of lower mechanical complexity.

4.4 LIMITATIONS OF THE EXPERIMENTAL APPROACH

Interpretation of the results of this thesis should take into account the experimental limitations inherent in the developed platform and adopted protocol. The analysis was based on kinematic indicators extracted from crank angular position, including number of complete cycles, mean cadence, temporal regularity and kinematic score. The observed results therefore do not represent direct measurements of torque, muscle force, mechanical power, physiological fatigue or absolute biomechanical efficiency.

The absence of torque or force sensors on the pedal limits the mechanical interpretation of the stimulation angular ranges suggested by the neural network. Although the results indicate improved pedalling continuity and cadence after adjustment of these ranges, it is not possible to state that the resulting configurations correspond to the intervals of greatest positive net torque at the crank. Such an analysis would require supplementary instrumentation, such as shaft torque transducers, instrumented pedals or load cells coupled to the mechanical system.

Another limitation concerns the size of the experimental dataset used for artificial-intelligence modelling. The MLP was used as an auxiliary regression and recommendation tool, but the small number of trials restricts generalisation of the results. The suggested configurations should therefore be interpreted as candidates valid for the evaluated experimental scenario, rather than as a universal solution applicable to different users, neurological injury levels, bicycle geometries or states of muscle fatigue.

Personalisation of the angular ranges was performed offline. Trial data were processed, classified and used to generate new configurations in discrete testing stages. The supervised-learning model therefore did not operate as an online adaptive controller and did not dynamically compensate for time-varying phenomena during trial execution, such as progressive fatigue, changes at the electrode–tissue interface or instantaneous cadence fluctuations.

In addition, the experimental tests were concentrated in an indoor environment using the trike coupled to a training roller. This condition favours repeatability and operational safety but does not fully reproduce disturbances present during real travel, such as surface irregularities, variable rolling resistance and additional stability demands. Transfer of the suggested configurations to an outdoor environment therefore requires future validation using specific metrics of speed, distance, pedalling continuity and operational safety.

Despite these limitations, the adopted approach was appropriate to the central objective of this thesis: consolidating an instrumented and traceable platform capable of relating stimulation configurations to observed kinematic performance. The main contribution of this study lies in structuring this experimental infrastructure, which enables patterns to be compared, trials to be ranked and dependence on purely empirical stimulation adjustment in FES-Cycling systems to be reduced.

4.5 CHAPTER SUMMARY

This chapter presented the experimental results of the FES-Cycling platform and discussed the association between stimulation angular ranges and pedalling kinematic performance. The analysis showed that the platform could distinguish configurations with lower and higher movement continuity, while keeping the interpretation restricted to kinematic indicators such as complete cycles, cadence and kinematic score.

Among the initial tests, Ti7 exhibited the best performance, whereas Ti6 had the lowest pedalling continuity. After the neural-network inferences, tests T8 and T9 improved relative to the best initial scenario, with T9 achieving the best kinematic performance among the evaluated trials. Since maximum stimulation amplitude was maintained at 34 mA, the observed improvement was interpreted, under the evaluated conditions, as being mainly associated with readjustment of the angular ranges.

The discussion positioned the proposed approach as an offline, data-driven experimental strategy to support initial stimulation personalisation. The methodology does not replace torque-based analyses, biomechanical models or real-time adaptive control, but it provides a traceable basis for comparing configurations and guiding new test conditions.

The identified limitations, particularly the absence of direct measurements of torque, muscle force, mechanical power and physiological fatigue, delimit the scope of the results and guide future work. The next chapter presents the general conclusions of the thesis and the main directions for continuing the research.

5 GENERAL CONCLUSIONS AND FUTURE WORK

5.1 GENERAL CONCLUSIONS

This thesis presented the development, integration and experimental evaluation of a multichannel FES-Cycling system using inertial feedback of crank angular position. The angular position was used as the closed-loop feedback variable to synchronise FES-channel activation with the stimulation ranges defined throughout the pedalling cycle.

The platform integrated inertial sensing, an embedded central-processing unit, FES modules, a manual intensity-control interface, an emergency stop and structured experimental data logging. This integration associated the kinematic response of each trial with the angular stimulation ranges applied, providing a traceable basis for comparing different muscle-activation configurations.

The central hypothesis was evaluated from a technical and experimental perspective. The results indicated that crank-angle feedback was sufficient to organise FES-channel activation in synchrony with the pedalling cycle and to distinguish stimulation configurations through kinematic indicators. The extracted metrics, including complete cycles, mean cadence, angular-velocity regularity, angular periodicity and the kinematic score, enabled objective ranking of the evaluated experimental conditions.

The artificial-intelligence stage was evaluated as an offline tool to support personalisation of stimulation ranges. An MLP neural network estimated candidate configurations from kinematic descriptors extracted from the trials. Under the evaluated conditions, the configurations tested after inference showed more favourable kinematic performance than the initial tests, including increased mean cadence, more complete cycles and a higher kinematic score. Because the study used a sequential single-participant design, these results do not establish that the neural network itself caused the improvement; they show that the offline inference-and-testing procedure was associated with the selection of favourable configurations within the evaluated set.

Overall, the proposed system met the design requirements defined in this thesis and provided a modular, traceable and comparatively low-complexity experimental infrastructure for data-driven FES-Cycling studies. Its principal contribution lies in integrating crank-angle feedback, multichannel stimulation, structured data acquisition and computational support for stimulation-range personalisation.

5.2 MAIN CONTRIBUTIONS OF THE THESIS

i. **Angular-feedback closed-loop architecture:** a functional FES-Cycling architecture in which instantaneous crank position, estimated by inertial sensing, synchronises FES-channel activation with predefined stimulation ranges.

ii. **Integrated electronic platform:** development and integration of an experimental platform based on a recumbent tricycle, comprising inertial acquisition, embedded processing, manual intensity adjustment, emergency stopping and multichannel FES modules.

iii. **Structured acquisition and data traceability:** an experimental protocol for recording time, crank position, stimulation ranges and trial parameters, enabling correspondence between the applied configuration and the observed kinematic response.

iv. **Kinematic-performance metrics:** definition and application of quantitative indicators for movement continuity, complete cycles, mean cadence, angular periodicity, angular-velocity regularity and the kinematic score.

v. **Offline artificial-intelligence personalisation:** application of an MLP neural network to support estimation and personalisation of stimulation ranges from kinematic descriptors, reducing reliance on exclusively empirical adjustment.

Together, these contributions provide an experimental basis for making FES-Cycling stimulation configuration more measurable, traceable and data-informed.

5.3 LIMITATIONS OF THE STUDY

The conclusions should be interpreted within the adopted experimental scope. The evaluation focused on the technical, operational and kinematic performance of the platform; it therefore does not constitute direct evidence of clinical functional gain, reduced physiological fatigue, longitudinal therapeutic benefit or absolute biomechanical efficiency.

The system did not use direct measurements of torque, pedal force or mechanical power as primary control variables. Consequently, the suggested ranges cannot be assumed to correspond to intervals of maximum positive net torque. The interpretation remains linked to kinematic indicators derived from crank angular position.

Artificial-intelligence personalisation was performed offline. The neural network did not act as a real-time adaptive controller; its outputs were treated as candidate configurations for experimental evaluation. This choice improved traceability but limited immediate compensation for time-varying phenomena such as progressive muscle fatigue and changes in neuromuscular response during a session.

The experimental dataset used to train and evaluate the neural network was small. Although the post-inference configurations showed improved performance in the evaluated trials, a larger and more diverse dataset is required to investigate generalisation across participants, neuromotor conditions and mechanical configurations.

Finally, the results are associated with the particular platform geometry, module arrangement, indoor training-roller environment, stimulated muscle groups and electrical parameters used. Changes to these factors may alter the observed kinematic response.

5.4 FUTURE WORK

Future work should expand the experimental dataset to include more participants, different neuromotor profiles and a wider range of angular configurations. This would permit a stronger assessment of personalisation robustness and model generalisation.

Complementary kinetic instrumentation, such as torque sensors, load cells or instrumented pedals, should also be considered. These measurements would relate the suggested angular ranges not only to kinematic performance but also to the effective mechanical contribution of the stimulated muscles, enabling more direct biomechanical validation.

Another direction is the development of real-time adaptive-control strategies. The present architecture already integrates angular sensing, FES activation and structured trial logging. Future versions could use cadence, angular regularity, fatigue estimates or mechanical metrics as feedback variables for automatically adjusting current amplitude, pulse width or angular-range limits during a session.

The MLP could be compared with regularised regression, probabilistic models, evolutionary algorithms, reinforcement learning and hybrid approaches incorporating biomechanical knowledge. Such comparisons would help identify methods suited to different dataset sizes, computational constraints and personalisation objectives.

From an electronic perspective, future work may improve inter-module communication, circuit encapsulation, connector standardisation, electrical protection and real-time monitoring. These improvements would increase operational reliability during longer trials and under less controlled conditions.

Finally, the platform should be evaluated in dynamic environments and longer-duration protocols. Real travel, outdoor tracks and longitudinal training studies could reveal the response to mechanical disturbances, changing effort, accumulated fatigue and user adaptation to assisted cycling.

5.5 FINAL REMARKS

The developed system showed that inertial feedback of crank angular position can provide a practical basis for synchronising functional electrical stimulation in FES-Cycling. The platform supported traceable trial logging, comparison of stimulation configurations and computational assistance for personalising angular ranges.

The proposed approach moves stimulation adjustment from a predominantly empirical procedure towards a data-informed experimental strategy. Despite the limitations associated with the absence of direct torque measurements, the size of the experimental dataset and offline personalisation, the results establish a consistent engineering foundation for more adaptive, traceable and personalised FES-Cycling systems.

REFERENCES

BAPTISTA, R.; SIJOBERT, B.; COSTE, C. A. New approach of cycling phases detection to improve FES-pedaling in SCI individuals. **IEEE/RSJ International Conference on Intelligent Robots and Systems**, p. 5181–5186, 2018. Cited 2 times on pages 38 and 40.

BELLMAN, M. J. *et al.* Switched control of cadence during stationary cycling induced by functional electrical stimulation. **IEEE Transactions on Neural Systems and Rehabilitation Engineering**, v. 24, n. 12, p. 1373–1383, 2016. Cited 4 times on pages 24, 29, 36, and 37.

BELLMAN, M. J. *et al.* Automatic control of cycling induced by functional electrical stimulation with electric motor assistance. **IEEE Transactions on Automation Science and Engineering**, v. 14, n. 2, p. 1225–1234, 2017. Cited 4 times on pages 38, 40, 41, and 42.

BÓ, A. P. L. *et al.* Cycling with spinal cord injury: A novel system for cycling using electrical stimulation for individuals with paraplegia, and preparation for cybathlon 2016. **IEEE Robotics and Automation Magazine**, v. 24, n. 4, p. 58–65, 2017. Cited on page 29.

BUSSADOR, A.; CASELLA, A. V.; NOHAMA, P. Eletroestimulador multifunções microcontrolado. In: **Anais do IV Fórum Nacional de Ciência e Tecnologia em Saúde**. Curitiba, PR: [s.n.], 1998. p. 179–180. Cited on page 35.

CACHO, E. W. A. **O efeito do treino de marcha com estimulação elétrica neuromuscular na atividade eletromiográfica de pacientes paraplégicos**. 2004. 92 p. Dissertação (Mestrado em Ciências da Cirurgia) — Universidade Estadual de Campinas, Campinas, 2004. Cited on page 23.

CASELLA, A. V.; BUSSADOR, A.; NOHAMA, P. Eletroestimulador eletrônico bifásico microcontrolado. In: **Memoria de Trabajos Científicos Mazatlán 98**. Mazatlán, México: [s.n.], 1998. p. 772–775. Cited on page 35.

COELHO-MAGALHÃES, T.; COSTE, C. A.; RESENDE-MARTINS, H. A novel functional electrical stimulation-induced cycling controller using reinforcement learning to optimize online muscle activation pattern. **Sensors**, v. 22, n. 23, p. 9126, 2022. Cited 4 times on pages 44, 45, 87, and 88.

COELHO-MAGALHÃES, T. *et al.* Development of a high-power capacity open source electrical stimulation system to enhance research into FES-assisted devices: Validation of FES cycling. **Sensors**, v. 22, n. 2, p. 531, 2022. Cited 8 times on pages 29, 30, 32, 35, 36, 37, 38, and 40.

COUSIN, C. A. *et al.* Closed-loop cadence and instantaneous power control on a motorized functional electrical stimulation cycle. **IEEE Transactions on Control Systems Technology**, v. 28, n. 6, p. 2276–2291, 2020. Cited 8 times on pages 24, 29, 32, 37, 38, 40, 41, and 42.

COUSIN, C. A. *et al.* Controlling the cadence and admittance of a functional electrical stimulation cycle. **IEEE Transactions on Neural Systems and Rehabilitation Engineering**, v. 27, n. 6, p. 1181–1192, 2019. Cited 2 times on pages 41 and 42.

D'Ancona, C. A. L. *et al.* Impacto da marcha com estimulação elétrica neuromuscular no perfil urodinâmico em pacientes com lesão raquimedular cervical alta. **Einstein (São Paulo)**, v. 8, n. 3, p. 325–328, 2010. Cited on page 23.

DUENAS, V. H. *et al.* Distributed repetitive learning control for cooperative cadence tracking in functional electrical stimulation cycling. **IEEE Transactions on Cybernetics**, v. 50, n. 3, p. 1084–1095, 2020. Cited 2 times on pages 41 and 42.

FARHOUD, A.; ERFANIAN, A. Fully automatic control of paraplegic FES pedaling using higher-order sliding mode and fuzzy logic control. **IEEE Transactions on Neural Systems and Rehabilitation Engineering**, v. 22, n. 3, p. 533–542, 2014. Cited 2 times on pages 41 and 42.

FARIA, U. d. C. **Implementação de um sistema de geração de marcha para pacientes com lesões medulares**. 2006. Tese (Doutorado em Engenharia Elétrica) — Universidade Estadual Paulista Júlio de Mesquita Filho, Ilha Solteira, 2006. Cited on page 35.

FARIA, U. d. C.; CARVALHO, A. A. d. Estimulador neuromuscular telemétrico bidirecional com detector de erros. In: **Anais do III Congresso Latino-Americano de Engenharia Biomédica**. João Pessoa, PB: [s.n.], 2004. v. 1, p. 421–424. Cited on page 35.

FARIA, U. d. C.; CARVALHO, A. A. d.; NITATORI, E. H. Estimulador neuromuscular funcional de 16 canais microcontrolado e portátil. In: **Anais do III Congresso Latino-Americano de Engenharia Biomédica**. João Pessoa, PB: [s.n.], 2004. v. 1, p. 417–420. Cited on page 35.

GAIOTTO, M. d. C. C. **Estimulador elétrico neuromuscular bifásico com saída em ponte H isolada eletricamente**. 2012. 124 p. Dissertação (Mestrado em Engenharia Elétrica e Informática Industrial) — Universidade Tecnológica Federal do Paraná, Curitiba, 2012. Cited on page 35.

GFÖHLER, M.; LUGNER, P. Dynamic simulation of FES-cycling: Influence of individual parameters. **IEEE Transactions on Neural Systems and Rehabilitation Engineering**, v. 12, n. 4, p. 398–405, 2004. Cited 3 times on pages 37, 38, and 41.

GOBBO, D. P. **Implementação de um circuito conversor de Tensão Corrente (V-I) para utilização em FES (Estimulação Elétrica Funcional)**. 2021. Monografia (Trabalho de conclusão de curso em Engenharia Elétrica) — UNESP, 2021. Cited on page 35.

GUILLOU, R. L. *et al.* A novel framework for quantifying accuracy and precision of event detection algorithms in FES-cycling. **Sensors**, v. 21, n. 13, p. 4571, 2021. Cited 2 times on pages 38 and 40.

HERNÁNDEZ, P. M. P. **Desenvolvimento de um sistema embarcado para ciclismo assistido por eletroestimulação – FES-Cycling**. 2022. 75 p. Dissertação (Mestrado em Engenharia Elétrica) — Universidade Estadual Paulista Júlio de Mesquita Filho, Ilha Solteira, 2022. Cited 2 times on pages 35 and 54.

HUNT, K. J. *et al.* On the efficiency of FES cycling: A framework and systematic review. **Technology and Health Care**, v. 20, n. 5, p. 395–422, 2012. Cited 8 times on pages 23, 29, 30, 31, 32, 35, 39, and 41.

IDSØ, E. S. **Development of a mathematical model of a rider-tricycle system**. Trondheim, Norway, 2002. Cited on page 36.

JUNIOR, A. C. **Restauração da Locomoção em Paraplégicos e Tetraplégicos com Sistemas Baseados em Estimulação Elétrica Neuromuscular**. 1992. Conferência. Cited on page 23.

JUNQUEIRA, M. V. N. **Eletroestimulador funcional de oito canais com malha de realimentação utilizando controlador digital**. 2013. 102 p. Dissertação (Mestrado em Engenharia Elétrica) — Universidade Estadual Paulista Júlio de Mesquita Filho, Ilha Solteira, 2013. Cited 2 times on pages 34 and 35.

JUNQUEIRA, M. V. N. *et al.* Estimulador elétrico neuromuscular microcontrolado. In: **Anais do XXIII Congresso Brasileiro de Engenharia Biomédica**. Porto de Galinhas, PE: [s.n.], 2012. v. 1, p. 1391–1395. Cited on page 35.

JUNQUEIRA, M. V. N. *et al.* Desenvolvimento de um eletroestimulador funcional de oito canais para aplicação com malha de realimentação utilizando controlador digital. In: **Actas del VII Congreso Iberoamericano de Tecnologías de Apoyo a la Discapacidad**. Santo Domingo, República Dominicana: [s.n.], 2013. Cited on page 35.

KLEIN, G. F. **Eletroestimulação Funcional em Pacientes com Lesão Medular**. 2001. Monografia (Monografia de Aperfeiçoamento/Especialização em Fisioterapia) — Centro Universitário Campos de Andrade, 2001. Cited on page 23.

LYNCH, C. L.; POPOVIC, M. R. Functional electrical stimulation. **IEEE Control Systems Magazine**, v. 28, n. 2, p. 40–50, 2008. Cited 6 times on pages 23, 28, 29, 30, 31, and 32.

MAFFIULETTI, N. A. Physiological and methodological considerations for the use of neuromuscular electrical stimulation. **European Journal of Applied Physiology**, v. 110, n. 2, p. 223–234, 2010. Cited 4 times on pages 29, 30, 31, and 32.

NOHAMA, P. Sistema nmes multicanal de dupla modulação controlado por computador. In: **Anais do III Fórum Nacional de Ciência e Tecnologia em Saúde**. Campos do Jordão, SP: [s.n.], 1996. Cited on page 35.

PAPCKE, C. *et al.* Investigation of the relationship between electrical stimulation frequency and muscle frequency response under submaximal contractions. **Artificial Organs**, v. 42, n. 6, p. 655–663, 2018. Cited on page 30.

PECKHAM, P. H.; KNUTSON, J. S. Functional electrical stimulation for neuromuscular applications. **Annual Review of Biomedical Engineering**, v. 7, n. 1, p. 327–360, 2005. Cited 6 times on pages 23, 28, 29, 30, 31, and 32.

PEDRO, R. N. *et al.* Perfil de resposta urodinâmica em pacientes submetidos à eletroestimulação para reabilitação motora (eenm) pós-trauma raquimedular alto. In: **30º Congresso Brasileiro de Urologia e 4º Congresso Brasileiro de Enfermagem em Urologia e 1º Encontro de Fisioterapia nas Disfunções Miccionais**. Brasília: [s.n.], 2005. v. 30, p. 171–171. Cited on page 23.

PENG, C.-W. *et al.* Review: Clinical benefits of functional electrical stimulation cycling exercise for subjects with central neurological impairments. **Journal of Medical and Biological Engineering**, v. 31, n. 1, p. 1–11, 2011. Cited 3 times on pages 23, 35, and 39.

PERES, A. B. *et al.* Validating Predictive Simulation-Derived Electrical Stimulation Cycling in a Person with Spinal Cord Injury. In: **2025 International Conference on Rehabilitation Robotics (ICORR)**. [S.l.: s.n.], 2025. p. 1245–1250. Cited 2 times on pages 46 and 47.

PERKINS, T. A. *et al.* Control of leg-powered paraplegic cycling using stimulation of the lumbo-sacral anterior spinal nerve roots. **IEEE Transactions on Neural Systems and Rehabilitation Engineering**, v. 10, n. 3, p. 158–164, 2002. Cited on page 35.

PRADO, T. A. **Implementação de um controlador PID embarcado para o controle em malha fechada de um estimulador neuromuscular funcional**. 2009. 77 p. Dissertação (Mestrado em Engenharia Elétrica) — Universidade Estadual Paulista Júlio de Mesquita Filho, Ilha Solteira, 2009. Cited on page 35.

RODRÍGUEZ, J. E. B. **Estimulador elétrico funcional com utilização de ponte H e fonte de corrente no estágio de potência**. 2016. Dissertação (Mestrado em Engenharia Elétrica) — Universidade Estadual Paulista Júlio de Mesquita Filho, Ilha Solteira, 2016. Cited 2 times on pages 34 and 35.

RODRÍGUEZ, J. E. B. *et al.* Estimulador elétrico funcional utilizando ponte h no estágio de potência. In: **Anais do XXV Congresso Brasileiro de Engenharia Biomédica**. Foz do Iguaçu, PR: [s.n.], 2016. Cited on page 35.

SANCHES, M. A. A. **Sistema eletrônico para geração e avaliação de movimentos em paraplégicos**. 2013. 184 p. Tese (Doutorado em Engenharia Elétrica) — Universidade Estadual Paulista Júlio de Mesquita Filho, Ilha Solteira, 2013. Cited on page 35.

SANNA, N. *et al.* A sensorized FES-cycling system to quantify training performance and optimize stimulation strategies. **Proceedings of the IEEE International Conference on Flexible and Printable Sensors and Systems**, p. 1–4, 2021. Cited 5 times on pages 32, 36, 37, 38, and 40.

SANNA, N. *et al.* Evaluating the health and fitness benefits of a 6-month FES-cycling program on a recumbent trike for individuals with motor complete SCI: a pilot study. **Journal of NeuroEngineering and Rehabilitation**, v. 22, n. 1, p. 55, 2025. Cited on page 47.

SAVONA, D. *et al.* On the road to Cybathlon 2024: lessons learned from the Polimi FES-bike team. **Journal of NeuroEngineering and Rehabilitation**, v. 23, n. 1, p. 97, 2026. Cited 2 times on pages 46 and 47.

SCHMOLL, M. *et al.* Oida: An optimal interval detection algorithm for automatized determination of stimulation patterns for FES-cycling in individuals with SCI. **Journal of NeuroEngineering and Rehabilitation**, v. 19, p. 39, 2022. Cited 6 times on pages 39, 43, 44, 45, 87, and 88.

SCHMOLL, M. *et al.* FES-Cycling at the Cybathlon 2024: assessing accuracy of power-pedals for low power output in a virtual race scenario. **Journal of NeuroEngineering and Rehabilitation**, 2026. Cited 2 times on pages 46 and 47.

SCHUTTE, L. M. *et al.* Improving the efficacy of electrical stimulation-induced leg cycle ergometry: An analysis based on a dynamic musculoskeletal model. **IEEE Transactions on Rehabilitation Engineering**, v. 1, n. 2, p. 109–125, 1993. Cited on page 36.

SILVA, T. I. d. **Implementação de um sistema para geração e avaliação de movimentos em pacientes hemiplégicos**. 2007. 171 p. Tese (Doutorado em Engenharia Elétrica) — Universidade Estadual Paulista Júlio de Mesquita Filho, Ilha Solteira, 2007. Cited on page 35.

SILVA, T. I. d.; CARVALHO, A. A. d.; FARIA, U. d. C. Estimulador neuromuscular funcional controlado via USB. In: **Anais do IV IBERDISCAP – Congresso Iberoamericano sobre Tecnologias de Apoio a Portadores de Deficiência**. Vitória, ES: [s.n.], 2006. v. 2, p. MO102–MO117. Cited on page 35.

SOUSA, A. C. C. de *et al.* A comparative study on control strategies for FES cycling using a detailed musculoskeletal model. **IFAC-PapersOnLine**, Elsevier, v. 49, n. 32, p. 204–209, 2016. Cited on page 39.

SOUZA, D. C. d. *et al.* Power amplifier circuits for functional electrical stimulation systems. **Research on Biomedical Engineering**, v. 33, n. 2, p. 144–155, 2017. Cited 3 times on pages 31, 34, and 35.

SOUZA, F. A. d. **Fonte de Alimentação DC com Diferentes Tensões para Alimentar um Estimulador Elétrico Funcional de Oito Canais Utilizando Conversor CC–CC**. 2016. Trabalho de Conclusão de Curso em Engenharia Elétrica. Cited on page 35.

WANNAWAS, N.; FAISAL, A. A. Towards AI-controlled movement restoration: Learning FES-cycling stimulation with reinforcement learning. In: **Proceedings of the IEEE International Conference on Rehabilitation Robotics**. [S.l.: s.n.], 2023. p. 1–6. Cited 7 times on pages 41, 42, 43, 44, 45, 87, and 88.

ANNEX A – RESEARCH ETHICS COMMITTEE APPROVAL

UNIVERSIDADE FEDERAL DO MATO GROSSO DO SUL - UFMS

PARECER CONSUBSTANCIADO DO CEP

DADOS DO PROJETO DE PESQUISA

Título da Pesquisa: ASSOCIAÇÃO SIMULTÂNEA DA FOTOBIOMODULAÇAO, ESTIMULAÇAO ELÉTRICA FUNCIONAL E CICLISMO PARA AUMENTAR O DESEMPENHO FÍSICO E QUALIDADE DE VIDA

Pesquisador: Adalberto Vieira Corazza

Área Temática:

Versão: 1

CAAE: 69620023.4.0000.0021

Instituição Proponente: FUNDACAO UNIVERSIDADE FEDERAL DE MATO GROSSO DO SUL

Patrocinador Principal: Financiamento Próprio

DADOS DO PARECER

Número do Parecer: 6.116.684

Apresentação do Projeto:

Entre as técnicas utilizadas para reabilitação de pessoas com dificuldades motoras encontra-se a Estimulação Elétrica Funcional (FES, acrônimo de Functional Electrical Stimulation). Esta técnica consiste na utilização de pulsos elétricos de curta duração para gerar contrações nos músculos e produzir o movimento funcional. A fototerapia de baixa potência, por meio de Lasers e Diodo Emissor de Luz (LED, acrônimo de Light Emitting Diode), é utilizada na área desportiva como eficiente fotomodulador da fadiga física e otimizador do desempenho físico. Este trabalho estuda a aplicação da FES associado simultaneamente a LEDT no contexto do ciclismo assistido para reabilitação e esporte de adulto hígidos, idosos e paraplégicos. O presente estudo será dividido em duas fases. A primeira fase será composta por três grupos existentes (adulto hígido, idoso e lesado

medular) com 22 participantes em cada grupo, sendo realizado independentemente análises com dois tipos de posicionamentos dos eletrodos no quadríceps femoral (longitudinal e transversal ao ventre muscular) para eletroestimulação associados a duas doses de energia no quadríceps femoral durante dois meses de estudo placebo-controlado e teste clínico cruzado. Na segunda fase, os participantes serão divididos aleatoriamente em dois grupos, que realizarão o ciclismo em bicicleta ergométrica horizontal. O Grupo 1 será submetido ao ciclismo assistido com FES associado simultaneamente a LEDT. O Grupo 2 realizará somente ciclismo assistido com FES e

Endereço: Av. Costa e Silva, s/nº - Pioneiros ¿ Prédio das Pró-Reitorias ¿Hércules Maymone¿ ¿ 1º andar
Bairro: Pioneiros **CEP:** 70.070-900
UF: MS **Município:** CAMPO GRANDE
Telefone: (67)3345-7187 **Fax:** (67)3345-7187 **E-mail:** cepconep.propp@ufms.br